

Multicomponent Analysis by Surface Plasmon Resonance-based  
Immunosensor for Control of Food Hygiene

Tomomi Yamasaki

March 15, 2019

# Contents

List of abbreviations	...	1	
Introduction	...	3	
Chapter 1	Development of an Immunosensor Based on Surface Plasmon Resonance for Simultaneous Residue Analysis of Three Pesticides —Boscalid, Clothianidin, and Nitenpyram— in Vegetables	...	6
Chapter 2	Development of a Surface Plasmon Resonance-Based Immunosensor for Detection of 10 Major O-Antigens on Shiga Toxin-Producing <i>Escherichia coli</i> , with a Gel Displacement Technique to Remove Bound Bacteria	...	31
Chapter 3	Evaluation of a Surface Plasmon Resonance-Based Multiplex O-antigen Serogrouping for <i>Escherichia coli</i> using Eleven Major Serotypes of Shiga Toxin-Producing <i>E. coli</i>	...	54
Chapter 4	Specific Detection of c-Kit Expressed on Human Cell Surface by Immunosensor Based on Surface Plasmon Resonance	...	72
List of publications	...	81	
Acknowledgements	...	83	

## List of abbreviations

BSA	bovine serum albumin
CCD	charge-coupled device
CDC	Centres for Disease Control and Prevention
CFU	colony-forming units
DART	direct analyses in real time
dcELISA	direct competitive enzyme-linked immunosorbent assay
DCM	dichloromethane
DMSO	dimethyl sulfoxide
<i>E. coli</i>	<i>Escherichia coli</i>
EDC	1-ethyl-3-(3-dimethylaminopropyl)carbodiimide, hydrochloride
EHEC	enterohemorrhagic <i>E. coli</i>
ELISA	enzyme-linked immunosorbent assay
GdnHCl	guanidine hydrochloride
HEK293T	human embryonic kidney cell line
HPLC	high performance liquid chromatography
HRP	horseradish peroxidase
HUS	haemolytic uremic syndrome
IC <sub>20</sub>	20% inhibitory concentrations
IC <sub>50</sub>	50% inhibitory concentrations
IC <sub>80</sub>	80% inhibitory concentrations
IR	Infrared
LC-MS	liquid chromatography with mass spectrometry
MEG01s	human megakaryoblastic leukemia cell line

MoAb	monoclonal antibody
MRL	maximum residue limit
NHS	<i>N</i> -hydroxysuccinimide
NMR	nuclear magnetic resonance
PBS	phosphate buffered saline
PBS-T	PBS containing 0.1% Tween 20
PCR	polymerase chain reaction
PFGE	pulsed-field gel electrophoresis
PoAb	polyclonal antibody
RSD	relative standard deviation
RU	resonance unit
SDS	sodium dodecyl sulfate
SPR	surface plasmon resonance
STEC	Shiga toxin-producing <i>Escherichia coli</i>
TFA	trifluoroacetic acid

## Introduction

Immunoassay is used for various analyses in the field of food hygiene. An immunosensor based on surface plasmon resonance (SPR immunosensor) can measure antigen-antibody reaction without labeling of antibody and allows rapid multicomponent analysis. In this study, SPR immunosensors for analyzing pesticide residues and Shiga toxin-producing *Escherichia coli* (STEC) have been developed. Furthermore, a SPR immunosensor for detecting surface proteins of animal cells has also been developed. These immunosensors would be applicable to other researches and analyses on food hygiene and cell surface factors in the future. Four chapters of this study are summarized below.

### *Chapter 1. Simultaneous analysis of three pesticides*

Boscalid is a carboxamide fungicide which was introduced in 2002. Clothianidin and nitenpyram are neonicotinoid insecticides introduced in 2002 and 1995, respectively. These are representative pesticide widely used around the world. Since fungicides and insecticides are often used in the same time for agricultural crops, simultaneous analytical methods for their residues have been required. However, the enzyme-linked immunosorbent assay (ELISA), which is an immunoassay commonly used for their analysis, is usually used for a single component. We aimed to develop a SPR immunosensor capable of simultaneous measuring of these three pesticides, boscalid, clothianidin, and nitenpyram by using a monoclonal antibody to each pesticide.

A sensor chip with four independent flow channels was used. Three conjugates of derivatives of each pesticide with bovine serum albumin (BSA) and BSA as a control were immobilized on each of the flow channels, and the resultant sensor chip was attached to a SPR instrument. The monoclonal antibody against each pesticide and the standard solution of each

pesticide were all mixed, and the mixture was injected into the SPR instrument and measured. Each pesticide was specifically measured in the range of 15 ng/mL to 93 ng/mL for boscalid, 6.7 ng/mL to 27 ng/ml for clothianidin, and 7.3 ng/mL to 62 ng/ml for nitenpyram. Pesticides spiked to vegetables can be measured at recovery of 72% to 105% with a high correlation to the direct competitive ELISA. It was confirmed that the SPR immunosensor developed is applicable as a practical analytical method for pesticide residues.

### *Chapter 2. Simultaneous serotyping of E. coli*

STEC is identified by microbiology test including O antigen serotyping. Six type of O antigens, O26, O103, O111, O121, O145 and O157, are tested in Japan, and over 90% of STEC is covered. However, because there are infections by STEC with other O antigens, a method that can be serotyped simultaneously with other O antigens has been required. Then, a microarray type SPR immunosensor has been developed here, which is capable of simultaneous serotyping for ten types of O antigens including O91, O115, O128, and O159 added to the six types above.

Ten kind of antibodies were purified from commercially available rabbit antisera against each O antigens and immobilized on different positions of a sensor chip, and the resultant chip was attached to a SPR instrument. A suspension of *E. coli* was injected into the SPR instrument and analyzed. *E. coli* with respective O antigen could be serotyped within a minute.

Usually, regeneration of used chip was very difficult because of the removal of bound *E. coli* without impairing the reactivity of antibody immobilized. We have succeeded in the regeneration by introducing gelatin gel. Now the sensor chip is able to be used for repeated measurement over 100 times.

### *Chapter 3. Clinical application of the developed SPR immunosensor*

Clinical 188 isolates of STEC with eleven type of O antigens including O45 added to the

above 10 O antigens were examined by the SPR immunosensor, and the results were compared with it of the slide agglutination method which is the conventional method for O antigen serotyping.

The overall sensitivity of O antigen serotyping was 98.9%. The detection limits of all serotypes were distributed between  $1.1 \times 10^6$  CFU/mL and  $17.6 \times 10^6$  CFU/mL. It was concluded that the SPR immunosensor developed in chapter 2 is useful as a simultaneous and automated method for O antigen serotyping of STEC.

#### *Chapter 4 Detection of membrane protein c-Kit of animal cells*

C-Kit is a cell membrane receptor with tyrosine kinase activity, which converts extracellular signals received into intracellular signals and controls the proliferation, differentiation, survival, metabolism, and migration of cells. C-Kit is important as a tumor marker because it is known to be highly expressed in gastrointestinal stromal tumors, germinal cell tumors such as seminomas, malignant melanoma, acute myeloid leukemia, etc. SPR immunosensor is developed as a detection method of c-Kit expressed on cell surface.

A commercially available anti-c-Kit antibody was immobilized on the surface of the sensor chip, and the resultant sensor chip was attached to a SPR instrument. A suspension of human megakaryoblastic leukemia cell line (MEG01s) and human embryonic kidney cell line (HEK 293T) was injected into the SPR instrument and analyzed. Although c-Kit could be detected, nonspecific reactions were observed. However, it was greatly suppressed by adding gelatin into the antibody solution for immobilizing. In addition, gelatin was also helpful for the regeneration of a used sensor chip as described in chapter 2.

# **Chapter 1      Development of an Immunosensor Based on Surface Plasmon Resonance for Simultaneous Residue Analysis of Three Pesticides —Boscalid, Clothianidin, and Nitenpyram— in Vegetables**

## **Abstract**

A simultaneous immunosensor based on surface plasmon resonance (SPR) was developed for determination of 3 pesticides - boscalid, clothianidin and nitenpyram - instead of the direct competitive enzyme-linked immunosorbent assays (dcELISAs) widely used as individual determination methods. Carboxy groups that introduced compounds to their pesticides were designed, and conjugates of them and bovine serum albumin were immobilized onto separate channels of the same sensor chip. When a mixture of 3 monoclonal antibodies reacted to each pesticide, and 3 pesticides were injected into the SPR immunosensor, each channel showed specific reactivity at 15 – 93 ng/mL for boscalid, 6.7 – 27 ng/mL for clothianidin, and 7.3 – 62 ng/mL for nitenpyram. Recovery tests using vegetables spiked with a mixture of 3 pesticides showed good results: 75 – 90%, 88 – 104%, and 72 – 105%, respectively, with a high correlation to results of the dcELISAs. The SPR immunosensor would be useful for the determination of pesticide residues in vegetables.

## **Introduction**

Boscalid, 2-chloro-*N*-(4'-chlorobiphenyl-2-yl) nicotinamide, is a carboxamide fungicide that was introduced in 2002.<sup>1</sup> Both clothianidin [(*E*)-1-(2-chloro-1,3-thiazol-5-ylmethyl)-3-methyl-2-nitroguanidine] and nitenpyram [(*E*)-*N*-(6-chloro-3-pyridylmethyl)-*N*-ethyl-*N'*-methyl-2-nitrovinylidenediamine] are neonicotinoid insecticides introduced in 2002 and 1995, respectively.<sup>2,3</sup> Clothianidin is a modified derivative of nitenpyram, although they have different ring structures; clothianidin has a chlorothiazol ring, whereas nitenpyram has a chloropyridine

ring, as shown in Fig. 1.<sup>4</sup> Fungicides and insecticides are often applied simultaneously to agricultural fields when the plants are put to risks of fungal disease and insect damage, especially in hot and humid seasons. The combination of boscalid and clothianidin or nitenpyram is also applied widely to prevent fungal diseases and insect pests. It is important to monitor their residues simultaneously in agricultural products. The maximum residue limits (MRLs) in vegetables have been set to 1 – 40 mg/kg for boscalid, 0.2 – 40 mg/kg for clothianidin, and 0.2 – 5 mg/kg for nitenpyram in Japan, including some exceptional vegetables for which the ranges are lower.

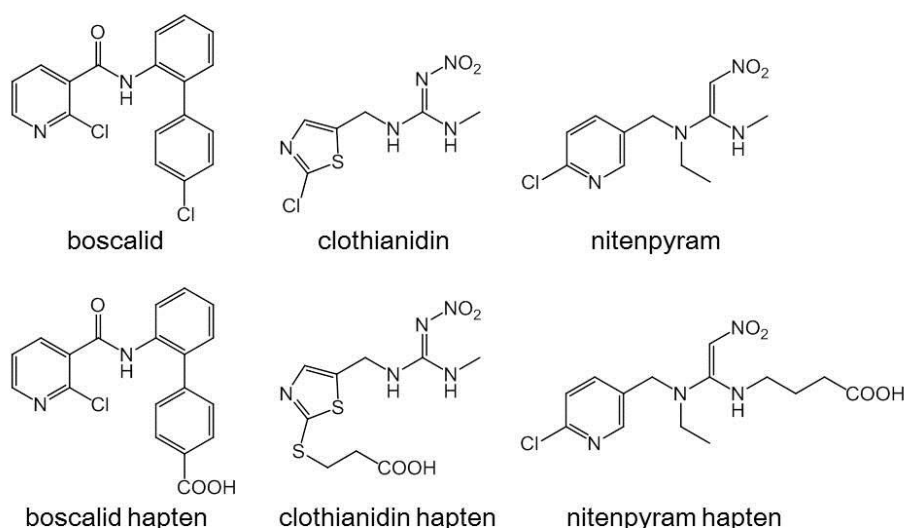


Fig. 1 Structure of boscalid, clothianidin, nitenpyram and their haptens.

Generally, boscalid is determined by gas or liquid chromatography by mass spectrometry.<sup>5-8</sup> Clothianidin and/or nitenpyram are determined by high-performance liquid chromatography (HPLC) with diode-array detection or by liquid chromatography with mass spectrometry (LC-MS).<sup>9-14</sup> Boscalid and clothianidin can be determined simultaneously by

multi-residue analysis using LC-MS.<sup>15-17</sup> These instrumental analyses are sensitive and accurate; however, these technologies are sophisticated, labor-intensive, and time-consuming.

Direct competitive enzyme-linked immunosorbent assays (dcELISAs) were developed for the monitoring of pesticide residues in vegetables as more simple and rapid methods compared to the above chromatography techniques, but of the single pesticide although simultaneous analysis is required in the field.<sup>18-20</sup> The development of simultaneous dcELISA for three pesticides was described previously.<sup>21</sup> Its reactivity was specific with each pesticide, but was difficult to put into practical use because optimization of the assay condition was complicated.

Immunosensors based on electrochemistry have been developed to determine pesticides in foods.<sup>22-24</sup> Immunosensors based on surface plasmon resonance (SPR immunosensors) have also been developed to determine pesticides.<sup>20,25-27</sup> Since SPR immunosensors especially enable real-time monitoring of the antigen-antibody interaction in contrast to the above dcELISAs and electrochemical immunosensors, they are expected to be applicable to pesticide residue analysis in fresh vegetables that will be quickly distributed. However, there have been no reports of any SPR immunosensor for the simultaneous and rapid analysis of pesticides, although it involves required techniques.

We hypothesized that a simultaneous SPR immunosensor would be developed if each of the antigen-antibody interactions showed no cross-reaction to the other target pesticides. In this study, we have described the successful development of a simultaneous SPR immunosensor to determine boscalid, clothianidin, and nitenpyram, with no cross-reaction among the pesticides, as their boscalid part is shown in Fig. 2. The design of the haptens has also been discussed in the context of developing simultaneous immunosensors.

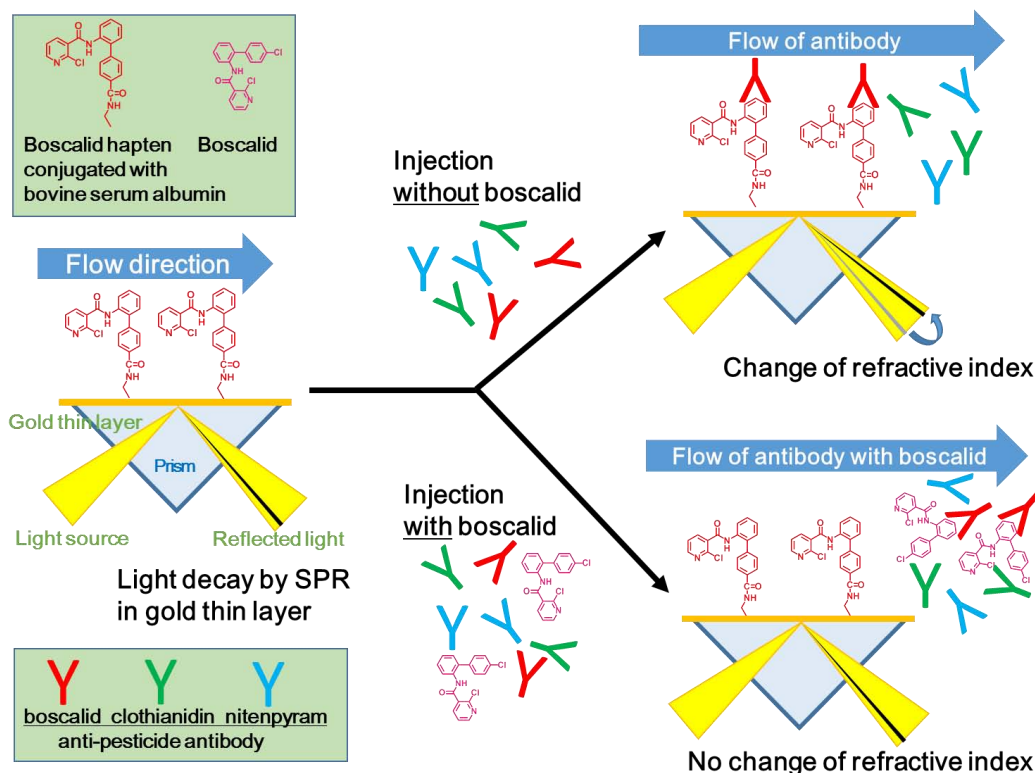


Fig. 2 Schematic illustration of boscalid determination on boscalid channel in the SPR immunosensor.

## Experimental

### Reagents and chemicals

Boscalid, benalaxyl, fenhexamid, tecloftalam, clothianidin, nitenpyram, imidacloprid, dinotefuran, thiacloprid, thiamethoxam were purchased from Wako Pure Chemical Industries, Ltd. (Osaka, Japan). Acetamiprid was purchased from Hayashi Pure Chemical Ind., Ltd. (Osaka, Japan). Bovine serum albumin (BSA: Prod. No. A7888) was purchased from Sigma-Aldrich Co. (St. Louis, MO, USA). Horseradish peroxidase (HRP) was purchased from Toyobo Co., Ltd. (Osaka, Japan). The anti-boscalid MoAb was prepared as described previously.<sup>20</sup> The anti-clothianidin MoAb and anti-nitenpyram MoAb were provided from Horiba Ltd. (Kyoto, Japan).<sup>18</sup> All other chemicals and reagents used were of analytical grade, and purchased from Wako Pure Chemical Industries, Ltd. or Nacalai Tesque, Inc.

### *Hapten design for boscalid and clothianidin*

The haptens for boscalid and clothianidin were synthesized as described previously.<sup>18,20</sup> Their structures were summarized in Fig. 1.

### *Hapten design for boscalid, clothianidin, and nitenpyram*

The hapten for nitenpyram was synthesized using the following scheme, referring to previous reports.<sup>28,29</sup> The structure was described in Fig. 1. All reactions were performed under an atmosphere of argon unless otherwise noted. Dichloromethane (CH<sub>2</sub>Cl<sub>2</sub>) was purchased from Kanto Chemical Co., Inc. (Tokyo, Japan). All reactions were monitored by thin layer chromatography that is glass plates pre-coated with silica gel (60 F254; layer thickness, 0.2 mm) purchased from Merck KGaA (Darmstadt, Deutschland). The products were visualized using irradiation with UV light or by treatment with a solution of phosphomolybdic acid or a solution of *p*-anisaldehyde. Flash column chromatography was performed using silica gel (Art. No. 7734) purchased from Merck KGaA. All other chemicals and reagents used were analytical grade, and purchased from Kanto Chemical Co., Inc..

Infrared (IR) spectra were measured on a JASCO FT/IR-4600 spectrometer. <sup>1</sup>H nuclear magnetic resonance (NMR) (500 MHz, 400 MHz) and <sup>13</sup>C NMR (125 MHz, 100 MHz) spectra were recorded on JEOL JNM-ECX500 and JEOL JNM-ECS400 spectrometers, respectively. Chemical shifts were reported as  $\delta$  values (ppm) relative to tetramethylsilane (0 ppm) and dimethyl sulfoxide (DMSO-d<sub>6</sub>; 2.50 ppm). Direct analyses in real time (DART) mass (positive mode) analyses were performed on a liquid chromatography-time-of-flight JMS-T100LP instrument. The overall synthesis scheme is summarized in Fig. 3.

#### *1) Synthesis of N-((6-chloropyridin-3-yl)methyl)ethanamine (2)*<sup>28</sup>

A solution of 2-chloro-5-(chloromethyl)pyridine (**1**) (972.1 mg, 6.0 mmol) in CH<sub>3</sub>CN (1.5

mL) was slowly added to a solution of ethanamine (3.865 g, 60 mmol, 70 wt% aqua.) in CH<sub>3</sub>CN (3.0 mL) over 25 min at 0 °C (in an ice-bath). The resulting mixture was stirred for 4 h at 0 °C (in an ice-bath), followed by the addition of H<sub>2</sub>O (10 mL). The product was extracted with CH<sub>2</sub>Cl<sub>2</sub> and dried with Na<sub>2</sub>SO<sub>4</sub>. The solvent was removed to give crude *N*-((6-chloropyridin-3-yl)methyl)ethanamine (**2**) (1.007 g) in 98% yield. **2** was used for the next step without further purification. **2**: <sup>1</sup>H NMR (500 MHz, CDCl<sub>3</sub>) δ 8.33 (d, 1H, *J* = 2.29 Hz, H-2 Py), 7.67 (dd, 1H, *J* = 2.29, 8.03 Hz, H-4 Py), 7.29 (d, 1H, *J* = 8.03 Hz, H-5 Py), 3.79 (s, 2H, -PyCH<sub>2</sub>NH-), 2.67 (q, 2H, *J* = 7.26 Hz, -NHCH<sub>2</sub>CH<sub>3</sub>), 1.13 (t, 3H, *J* = 7.26 Hz, -NHCH<sub>2</sub>CH<sub>3</sub>) ppm. <sup>13</sup>C NMR (125 MHz, CDCl<sub>3</sub>) δ 149.6, 149.0, 138.5, 134.7, 123.7, 50.0, 43.4, 14.9 ppm. High-resolution mass spectrometry (HRMS) (DART) *m/z*: calcd. for C<sub>8</sub>H<sub>12</sub>ClN<sub>2</sub> (M+1+) 171.0689, found 171.0682. IR (neat) 3418, 3087, 2968, 1458, 1104 cm<sup>-1</sup>.

## 2) Synthesis of

### *N*-((6-Chloropyridin-3-yl)methyl)-*N*-ethyl-1-(methylthio)-2-nitroethen-1-amine (**3**)<sup>28</sup>

*N*-((6-chloropyridin-3-yl)methyl)ethanamine (**2**) (1.00 g, 5.9 mmol) was dissolved in anhydrous EtOH (3.0 mL), followed by the addition of (2-nitroethene-1,1-diyl)bis(methylsulfane) (886.4 mg, 5.4 mmol). The resulting mixture was heated to reflux for 6 h, followed by continuous stirring for 17.5 h at room temperature. The mixture was refluxed again for 4.5 h and cooled to room temperature. The solvent was then removed. The residue was purified by column chromatography on silica gel (hexane/ethyl acetate = 3/1 → 1/1 → 1/3 v/v) to give *N*-((6-chloropyridin-3-yl)methyl)-*N*-ethyl-1-(methylthio)-2-nitroethen-1-amine (**3**) (616.3 mg) in 40% yield. **3**: <sup>1</sup>H NMR (400 MHz, CDCl<sub>3</sub>) δ 8.27 (d, 1H, *J* = 2.44 Hz, H-2 Py), 7.55 (dd, 1H, *J* = 2.44, 8.24 Hz, H-4 Py), 7.35 (d, 1H, *J* = 8.24 Hz, H-5 Py), 6.80 (s, 1H, -CHNO<sub>2</sub>), 4.69 (s, 2H, -PyCH<sub>2</sub>N-), 3.49 (q, 2H, *J* = 7.02 Hz, -NCH<sub>2</sub>CH<sub>3</sub>), 2.47 (s, 3H, -SCH<sub>3</sub>), 1.25 (t, 3H, *J* = 7.02 Hz, -NCH<sub>2</sub>CH<sub>3</sub>) ppm. <sup>13</sup>C NMR (125 MHz, CDCl<sub>3</sub>) δ 165.7, 151.2, 148.6, 137.9, 130.1,

124.5, 113.8, 53.1, 48.5, 17.7, 13.1 ppm. HRMS(DART)  $m/z$ : calcd. for  $C_{11}H_{15}ClN_3O_2S$  ( $M+1^+$ ) 288.0574, found 288.0549. IR (neat) 2976, 1519, 1388, 1258, 1106  $cm^{-1}$ .

3) Synthesis of *tert*-butyl 4-((1-(((6-chloropyridin-3-yl)methyl)(ethyl)amino)-2-nitrovinyl)amino)butanoate (**4**)<sup>29</sup>

A solution of *tert*-butyl 4-aminobutanoate hydrochloride (19.6 mg, 0.1 mmol) in  $CH_3CN$  (0.1 mL) was added drop-wise to a mixture of *N*-((6-chloropyridin-3-yl)methyl)-*N*-ethyl-1-(methylthio)-2-nitroethen-1-amine (28.8 mg, 0.1 mmol) and  $K_2CO_3$  (41.5 mg, 0.3 mmol) in dry  $CH_3CN$  (0.6 mL) at room temperature. The resulting mixture was stirred for 23 h at room temperature. The solvent was then removed and the residue was purified by column chromatography on silica gel (hexane/ethyl acetate = 2/1 → 1/1 → 1/0 → ethyl acetate/methanol = 1/1 v/v) to give *tert*-butyl 4-((1-(((6-chloropyridin-3-yl)methyl)(ethyl)amino)-2-nitrovinyl)amino)butanoate (**4**) (21.6 mg) in 54% yield. **4**:  $^1H$  NMR (500 MHz,  $CDCl_3$ )  $\delta$  9.56 (bs, 1H, -NH), 8.29 (d, 1H,  $J = 2.29$  Hz, H-2 Py), 7.56 (dd, 1H,  $J = 2.68, 8.03$  Hz, H-4 Py), 7.36 (d, 1H,  $J = 8.03$  Hz, H-5 Py), 6.52 (s, 1H, -CHNO<sub>2</sub>), 4.35 (s, 2H, -PyCH<sub>2</sub>N-), 3.40 (q, 2H,  $J = 6.88$  Hz, -NCH<sub>2</sub>CH<sub>3</sub>), 3.12 (q, 2H,  $J = 7.26$  Hz, -NCH<sub>2</sub>CH<sub>2</sub>CH<sub>2</sub>COO*t*-Bu), 2.36 (t, 2H,  $J = 6.88$  Hz, -NCH<sub>2</sub>CH<sub>2</sub>CH<sub>2</sub>COO*t*-Bu), 1.93-1.99 (m, 2H, -NCH<sub>2</sub>CH<sub>2</sub>CH<sub>2</sub>COO*t*-Bu), 1.44 (s, 9H, *t*-Bu), 1.18 (t, 3H,  $J = 6.88$  Hz, -NCH<sub>2</sub>CH<sub>3</sub>) ppm.  $^{13}C$  NMR (125 MHz,  $CDCl_3$ )  $\delta$  171.8, 162.1, 151.1, 148.6, 138.0, 130.2, 124.5, 103.8, 80.7, 49.8, 44.9, 44.6, 31.9, 27.9, 25.2, 12.0 ppm. HRMS(DART)  $m/z$ : calcd. for  $C_{18}H_{28}ClN_4O_4$  ( $M+1^+$ ) 399.1799, found 399.1799. IR (neat) 3452, 3131, 2977, 2934, 1724, 1517, 1366  $cm^{-1}$ .

4) Synthesis of nitenpyram hapten,

4-((1-(((6-chloropyridin-3-yl)methyl)(ethyl)amino)-2-nitrovinyl)amino)butanoic acid (**5**)<sup>29</sup>

A solution of *tert*-butyl 4-((1-(((6-chloropyridin-3-yl)methyl)(ethyl)amino)-2-nitrovinyl)amino)butanoate (**4**)

(17.2 mg, 0.043 mmol) in  $\text{CH}_2\text{Cl}_2$  (DCM; 0.43 mL) was treated with  $\text{CF}_3\text{COOH}$  (trifluoroacetic acid (TFA); 46  $\mu\text{L}$ ). The mixture was stirred for 23 h at room temperature. The solvent was removed and the residue was purified by column chromatography on silica gel (ethyl acetate/methanol = 15/1 $\rightarrow$ 8/1 v/v) to give the desired nitenpyram hapten,

4-((1-(((6-chloropyridin-3-yl)methyl)(ethyl)amino)-2-nitrovinyl)amino)butanoic acid (**5**) (13.4 mg) in 91% yield. **5**:  $^1\text{H NMR}$  (500 MHz,  $\text{DMSO-d}_6$ )  $\delta$  12.17 (bs, 1H,  $-\text{COOH}$ ), 8.67 (bs, 1H,  $-\text{NH}$ ), 8.34 (d, 1H,  $J = 2.29$  Hz, H-2 Py), 7.34 (dd, 1H,  $J = 2.29, 8.03$  Hz, H-4 Py), 7.51 (d, 1H,  $J = 8.03$  Hz, H-5 Py), 6.43 (s, 1H,  $-\text{CHNO}_2$ ), 4.51 (s, 2H,  $-\text{PyCH}_2\text{N}-$ ), 3.22-3.27 (m, 4H,  $-\text{NCH}_2\text{CH}_3$ ,  $-\text{NCH}_2\text{CH}_2\text{CH}_2\text{COOH}$ ), 2.23 (t, 2H,  $J = 7.26$  Hz,  $-\text{NCH}_2\text{CH}_2\text{CH}_2\text{COOH}$ ), 1.70-1.77 (m, 2H,  $-\text{NCH}_2\text{CH}_2\text{CH}_2\text{COOH}$ ), 1.11 (t, 3H,  $J = 7.26$  Hz,  $-\text{NCH}_2\text{CH}_3$ ) ppm.

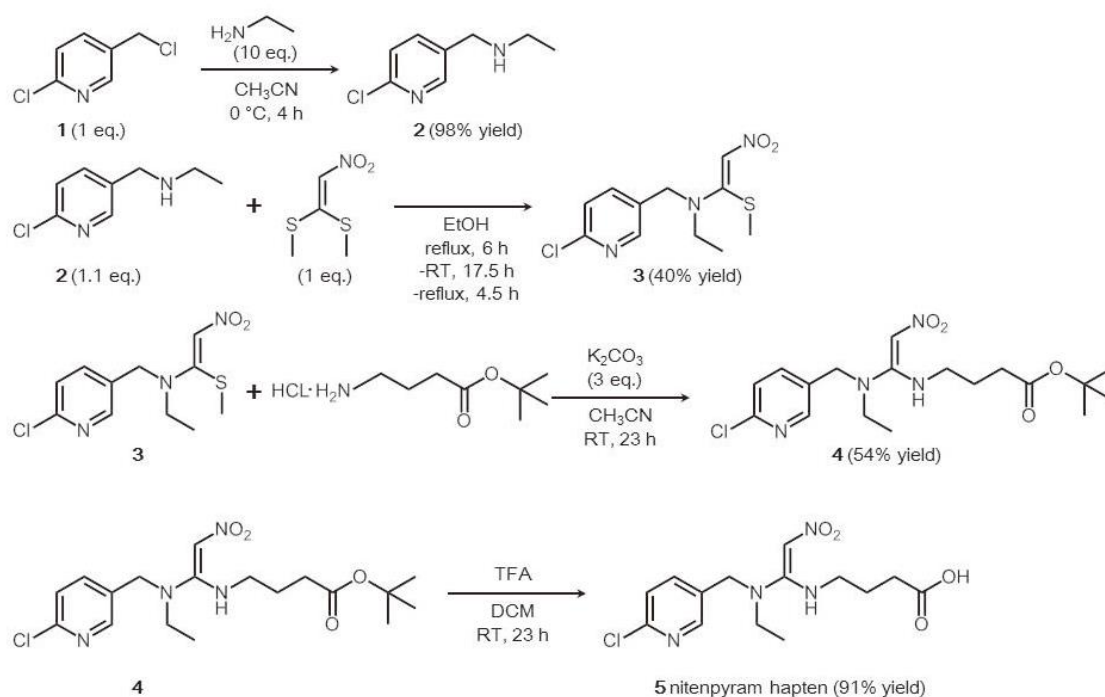


Fig. 3 Scheme of the nitenpyram hapten synthesis.

### *Preparation of hapten and protein conjugate*

Boscalid, clothianidin, and nitenpyram haptens were, respectively, conjugated to BSA and HRP, as described previously.<sup>20</sup>

### *Constitution of SPR immunosensor*

The SPR immunosensor comprised a commercially available microflow-type instrument (Biacore T200; GE Healthcare Europe, Munich, Germany), and its sensor chip had four channels coated with carboxymethyl dextran (CM5; GE Healthcare Europe), as described previously.<sup>20,27</sup>

#### *1) Preparation of the sensor chip for the three pesticides*

The sensor chip was placed in the instrument. The chip channels were rinsed with PBS containing 0.005% tween 20 for 600 s at 5  $\mu\text{L}/\text{min}$ . The carboxy groups in the channels were then activated by rinsing with a mixture of 80  $\mu\text{L}$  of EDC (400 mmol/L) and 80  $\mu\text{L}$  of NHS (100 mmol/L) dissolved in distilled water for 350 s at 5  $\mu\text{L}/\text{min}$ . The three kinds of hapten and BSA conjugates (40  $\mu\text{g}/\text{mL}$  each) dissolved in acetic acid buffer (10 mmol/L; pH 5.0) were respectively added to their respective channels for 360 s at 5  $\mu\text{L}/\text{min}$  to immobilize them onto the channels. The remaining channel was used for a negative control to permit deletion of the baseline noise. Ethanolamine (1 mol/L; pH 8.5) was allowed to flow for 350 s at 5  $\mu\text{L}/\text{min}$  to inactivate the residual carboxy groups. The prepared sensor was rinsed with running buffer (50 mmol/L phosphate buffer containing 75 mmol/L NaCl, 0.1% BSA, and 5% methanol; pH 7.0), and was then ready for use.

#### *2) Preparation of sample*

The pesticide standard solutions were prepared with 10% methanol to the following concentrations: boscalid and nitenpyram (3.1 – 200 ng/mL), clothianidin (1.6 – 100 ng/mL), dinotefuran (1.6 ng/mL – 10  $\mu\text{g}/\text{mL}$ ), thiacloprid (160 ng/mL – 100  $\mu\text{g}/\text{mL}$ ), and the other

pesticides (10 µg/mL). The pesticides were mixed at the same final concentrations for simultaneous analysis. By contrast, the anti-boscalid, anti-clothianidin, and anti-nitenpyram MoAbs were diluted to 15 µg mL<sup>-1</sup> with high ion strength phosphate buffered saline (modified PBS: 100 mmol/L phosphate, 150 mmol/L NaCl; pH7.0) containing 0.2% BSA. A mixture of the MoAbs was also prepared at the same final concentration. The pesticide standard solution or the diluent prepared from the vegetables (75 µL) was mixed with an equal volume of the MoAb solution (75 µL), and used as measurement samples.

### *3) Analysis conditions*

Measurement samples were allowed to flow serially through the first boscalid channel, the second clothianidin channel, and the last nitenpyram channel immobilized with each of the corresponding haptens and BSA conjugate for 180 s at 20 µL/min. The solution was continuously changed to the running buffer, and it was allowed to flow further for 180 s at 20 µL/min to obtain the *K<sub>d</sub>* values.

### *4) Regeneration of the sensor-chip*

After the reaction was complete, the sensor-chip was regenerated by removal of the bound MoAbs. GdnHCl (3.0 mol/L) in acetic acid (1.0 mol/L; pH 1.9) was allowed to flow initially for 60 s at 20 µL/min. After rinsing with distilled water for 60 s at 20 µL/min, the chips were rinsed with 0.2% SDS for 120 s at 20 µL/min to complete regeneration. The sensor chip was re-used after rinsing with running buffer.

### *5) Data processing*

Raw data were output as resonance units (RUs). A 0.1 degree refractive index shift by the SPR phenomenon was defined as 1000 RUs. The actual reaction signal was represented as the delta RU value at 180 s from the start of the reaction.

### *dcELISA*

dcELISA was performed as described previously.<sup>20</sup> The specific conditions for boscalid, clothianidin, and nitenpyram are described below. The anti-pesticide MoAbs were diluted with PBS (10 mmol/L phosphate, 150 mmol/L NaCl; pH7.0) to the following concentrations: anti-boscalid MoAb (500 ng/mL), anti-clothianidin MoAb (250 ng/mL), and anti-nitenpyram MoAb (125 ng/mL). The hapten and HRP conjugates were diluted with modified PBS containing 0.2% BSA to the following concentrations: 250 ng/mL for boscalid, 50 ng/mL for clothianidin, and 1000 ng/mL for nitenpyram. Pesticide standard solutions were prepared in 10% methanol to the following concentrations: boscalid (0.038 – 156 ng/mL), clothianidin (0.024 – 100 ng/mL), and nitenpyram (0.24 – 1000 ng/mL).

### *Preparation of vegetable samples*

A variety of vegetables belonging to different families, (broccoli (*Brassica oleracea var. italica*), cucumber (*Cucumis sativus L.*), lettuce (*Lactuca sativa L.*), spinach (*Spinacia oleracea L.*), tomato (*Solanum lycopersicum L.*), and Welsh onion (*Allium fistulosum L.*)) were purchased from a market in Kyoto city. dcELISAs, which are more sensitive than the SPR immunosensor, were used to confirm that they did not contain any boscalid, clothianidin, or nitenpyram. The vegetable samples (100 g) were homogenized in a blender. Pesticide mixtures dissolved in methanol (100  $\mu$ L) were spiked into the homogenized samples (5.0 g) in 50 mL screw-cap tubes at the final concentrations of boscalid, clothianidin, and nitenpyram: A) 2, 0.75, and 1.5  $\mu$ g/g; B) 4, 1.5, and 3  $\mu$ g/g; C) 8, 3, and 6  $\mu$ g/g, respectively. After standing for 30 min at room temperature, 25 mL of methanol was added to the homogenates. The tubes were shaken vigorously on a reciprocal shaker (Shaker SA320; Yamato Scientific Co., Ltd., Tokyo, Japan) for 30 min to extract the pesticides into the liquid phase. The extracts were centrifuged at 3000 rpm for 10 min at room temperature. The supernatants were diluted to 8.5-folds with distilled

water to prepare 10% methanol equivalent solutions. They were further diluted with 10% methanol to adjust the concentrations to the working range of the SPR immunosensor or the dcELISA. The diluents were used to prepare measurement samples.

## Results and Discussion

### *Hapten design*

For simultaneous analysis, measurement samples containing the three MoAbs and the three pesticides were allowed to flow serially through the boscalid, clothianidin, and nitenpyram channels immobilized with each of haptens and BSA conjugate. The hapten on one channel is therefore necessary to react with the corresponding MoAb only without any cross reaction on the other channels.

As shown in Fig. 1, boscalid has a structure different from that of clothianidin, but has the same 2-chloropyridine ring structure as nitenpyram. It is present in the basic structure at the *ortho*-position in boscalid, but at the *para*-position in nitenpyram. Generally, it is easy to raise MoAbs that recognize such a difference in the angle. We presumed that the haptens for boscalid would not react with the anti-nitenpyram MoAb. By contrast, the 2-chlorobenzene ring in the basic structure of the boscalid at the *para*-position is similar to the structure of the 2-chloropyridine ring in nitenpyram, which might make it difficult for a MoAb to recognize the difference. Therefore, the linker of boscalid was extended from the chlorine position of the 2-chlorobenzene ring to inhibit any possible cross-reaction.

Clothianidin and nitenpyram belong to the same neonicotinoid insecticide group. Clothianidin has a nitroguanidine structure that is similar to the nitrovinylidenediamine structure in nitenpyram. Thus, their haptens might react with MoAb raised against another hapten, resulting in a failure to develop a useful simultaneous SPR immunosensor. In a previous study, two kinds of haptens of the insecticide etofenprox, whose linker sites were on opposite sides (at

the ethoxy group and the phenoxybenzene group), induced different cross reactivity with the antibodies raised against the haptens.<sup>30</sup> Thus, we believed that the concept would be effective to develop a simultaneous SPR immunosensor. The clothianidin hapten was synthesized based on the published structure,<sup>18</sup> and then the linker for the nitenpyram hapten was introduced at the opposite side from clothianidin (Fig. 1).

As shown in Table 1, each of the haptens actually functioned in the constituted SPR immunosensor without any cross-reaction with the other MoAbs, when each of the MoAb solutions flowed serially through the first boscalid channel, the second clothianidin channel, and the last nitenpyram channel.

Table 1 Typical signal of anti-pesticide MoAbs onto each pesticide channel by the constituted SPR immunosensor

MoAb	Channel immobilized with hapten and BSA conjugate (delta RU)		
	Boscalid	Clothianidin	Nitenpyram
Anti-boscalid	450	0	0
Anti-clothianidin	2	1500	8
Anti-nitenpyram	0	3	310

#### *Determination of pesticides by the SPR immunosensor*

The anti-boscalid MoAb, the anti-clothianidin MoAb, and the anti-nitenpyram MoAb solutions were injected separately into the SPR immunosensor. The RU value of the MoAb solutions increased in a time-dependent manner, reaching 450 RU for boscalid, 1500 RU for clothianidin, and 310 RU for nitenpyram at 180 s from the reaction start point, as shown in Fig. 4A. The signals were returned to the baseline after washing with 3 kinds of regeneration buffers. The *K<sub>d</sub>* values, calculated from the time course results, were determined as  $2.9 \times 10^{-12}$  mol/L for boscalid,  $8.1 \times 10^{-12}$  mol/L for clothianidin, and  $7.7 \times 10^{-12}$  mol/L for nitenpyram. All of the

MoAbs showed high affinity to the corresponding hapten and BSA conjugate, as indicated by the  $K_d$  values. These high affinities are important to constitute an SPR immunosensor for the accurate determination of the pesticides.

The determination of each pesticide was initially examined using the SPR immunosensor. The signal produced between the hapten and BSA conjugate and the MoAb was inhibited by the corresponding pesticide in a concentration-dependent manner for all three pesticides, as shown in Figs. 4B – 4D. The inhibition curves were drawn using the signal data at 180 s from the reaction start point, as shown in Fig. 5. The 20%, 50%, and 80% inhibitory concentrations ( $IC_{20}$ ,  $IC_{50}$ , and  $IC_{80}$ ) were 15, 41, and 93 ng/mL for boscalid; 6.7, 15, and 27 ng/mL for clothianidin; and 7.3, 24, and 62 ng/mL for nitenpyram. The quantitative working ranges, defined as between the  $IC_{20}$  value and  $IC_{80}$  value, suggested that the SPR immunosensor was sufficiently sensitive to be applied to residue analysis of the target pesticides around the MRLs in the majority of vegetables.

The constituted SPR immunosensors were combined for the simultaneous analysis of their pesticides. A mixture of the three MoAbs was added to each pesticide, but also a mixture of their pesticides, and this mixture was injected into the SPR immunosensor. As shown in Fig. 5, the inhibition curves were almost identical to the above determination results for the individual MoAbs. The simultaneous SPR immunosensor could determine boscalid in the range of 15 – 93 ng/mL, clothianidin in the range of 6.7 – 27 ng/mL, and nitenpyram in the range of 7.3 – 62 ng/mL. This successful result could be attributed by the design of highly specific haptens that reacted only with the corresponding MoAb and by the use of high affinity MoAbs.

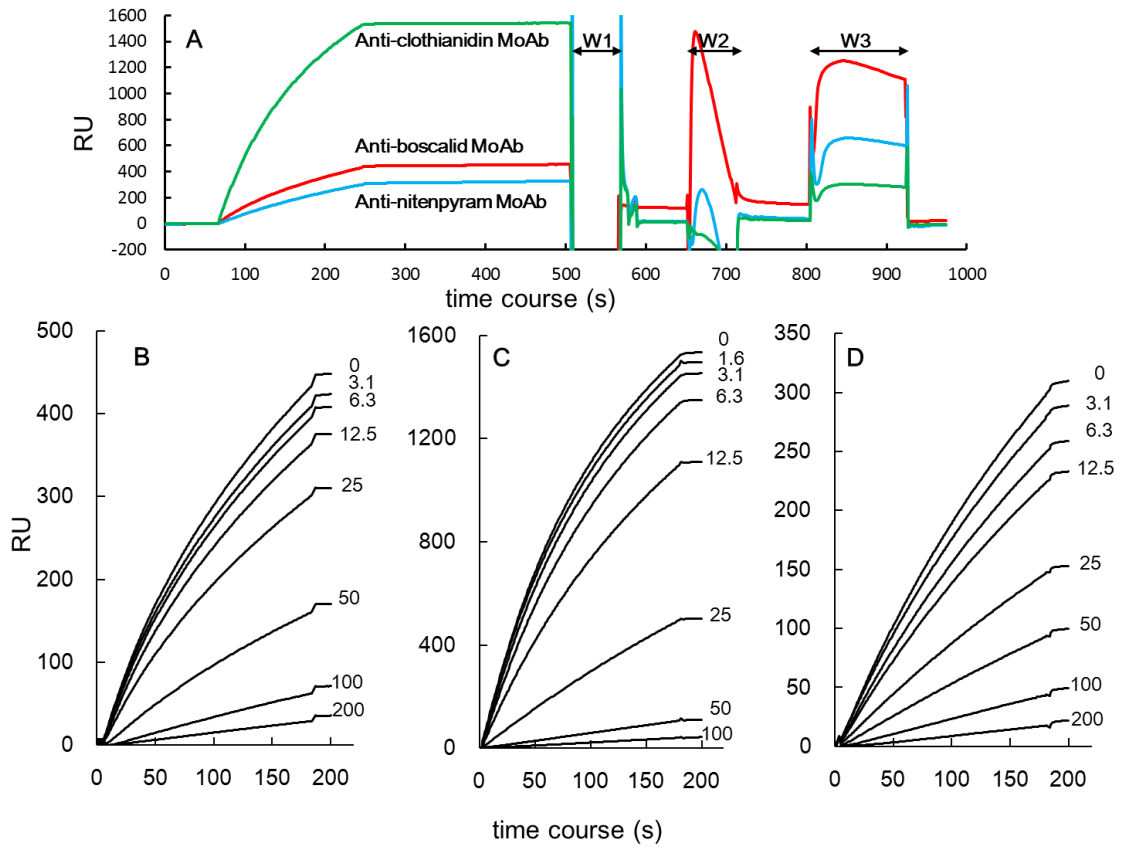


Fig. 4 Time course of anti-pesticide MoAbs reaction without the corresponding pesticides on each channel in SPR-immunosensor (A), and their signal reduction by the corresponding pesticides (ng/mL): (B) boscalid, (C) clothianidin, (D) nitenpyram. W1, W2, and W3 show regeneration steps by GdnHCl in acetic acid (pH 1.9), distilled water, and 0.2% SDS, respectively.

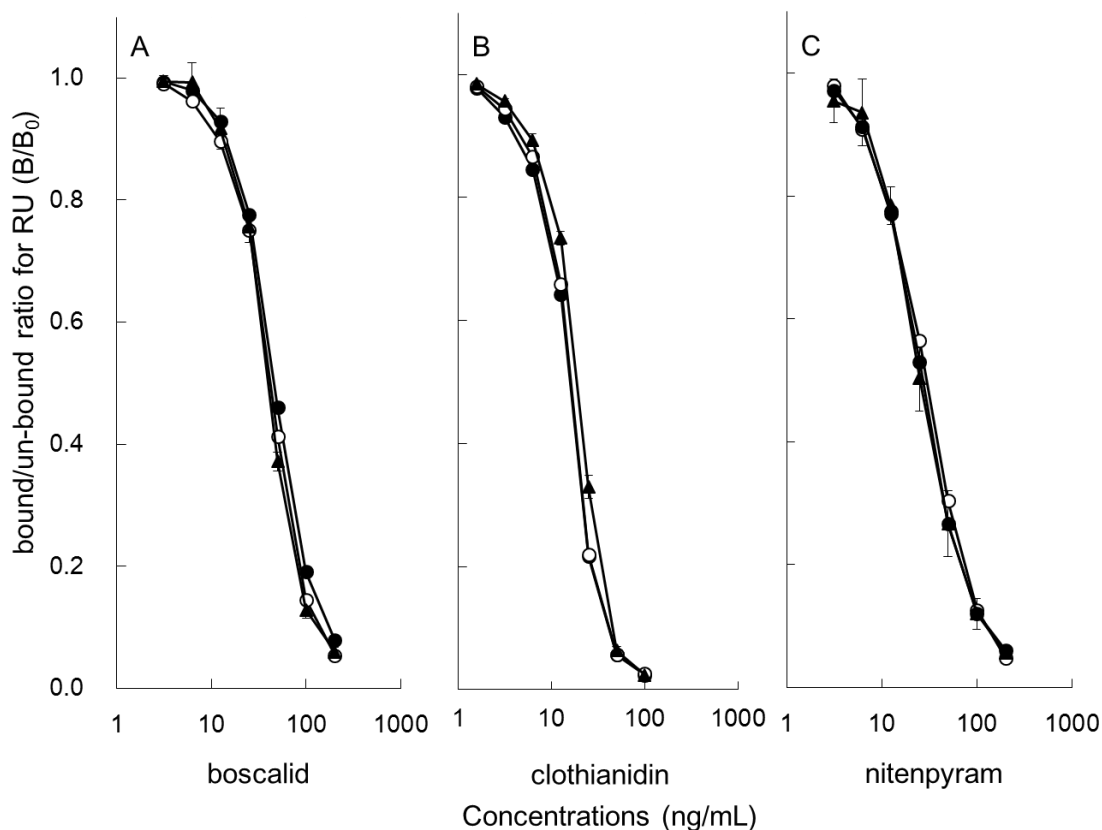


Fig. 5 Inhibition curves for each of the pesticides by SPR-immunosensor: (A) boscalid, (B) clothianidin, (C) nitenpyram. (●) shows inhibition curve for each of the MoAbs with the 1 pesticide, (○) shows inhibition curve for the mixture of 3 MoAbs with the 1 pesticide, and (▲) shows inhibition curve for the mixture of 3 MoAbs with 3 pesticides. Each data point is the mean of triplicate in independent examinations; error bars indicate  $\pm$  SD.

### Cross reactivity

The constituted SPR immunosensor was highly specific to boscalid, clothianidin, and nitenpyram. However, it was not clear whether other structurally related pesticides would cross-react in the SPR immunosensor. Therefore, the cross-reactivity of the anti-boscalid MoAb was examined using fenhexamid, tecloftalam, and benalaxyl, which belong to the same carboxamide

fungicide group. The cross-reactivity of anti-clothianidin and anti-nitenpyram MoAbs was examined using acetamiprid, imidacloprid, dinotefuran, thiacloprid, and thiamethoxam, which are all neonicotinoid insecticides. The three MoAbs were mixed, and the mixture was further mixed with each of the pesticides. After injection into the SPR immunosensor, each of the IC<sub>50</sub> values was obtained from inhibition curves drawn from the time course signal. The cross-reactivity (%) of the MoAbs was obtained from their ratio with the target pesticide. As described in Table 2, the sensor channel for boscalid was specific to boscalid. The sensor channel for nitenpyram was also specific to nitenpyram despite acetamiprid, imidacloprid, and thiacloprid having the 2-chloropyridine ring bound on the *para*-position like nitenpyram. It was speculated that the anti-nitenpyram MoAb used would recognize nitrovinylidenediamine *via* the 2-chloropyridine ring of nitenpyram, because the linker of the hapten was extended from the methyl amine, which exists on the opposite side from the 2-chloropyridine ring.

In contrast, the anti-clothianidin MoAb cross-reacted with dinotefuran at the same level as clothianidin. The cross-reactivity was 119%. Dinotefuran and clothianidin have a common structure: the 1,3-dimethyl-2-nitroguanidin group. The hapten linker of clothianidin was extended from the chlorine atom position of the thiazole ring, which exists on the opposite side of the nitroguanidin group, as shown in Fig. 1. We speculated that the anti-clothianidin MoAb must recognize this common structure.

Thus, the cross-reactivity examination suggested that the SPR immunosensor could determine dinotefuran in addition to boscalid, clothianidin, and nitenpyram. Dinotefuran, clothianidin, and nitenpyram, which belong to the same insecticide group, are not usually applied to an agricultural field at the same time. Thus, it was suggested that the constituted SPR immunosensor can determine boscalid and dinotefuran simultaneously, in addition to boscalid and clothianidin, or boscalid and nitenpyram.

Table 2 Cross-reactivity of the MoAbs with the structurally related pesticides by the SPR immunosensor

Pesticides examined	Cross-reactivity (%) of MoAbs		
	Anti-boscalid	Anti-clothianidin	Anti-nitenpyram
Boscalid	100 <sup>a</sup>	<0.18	<0.22
Clothianidin	<0.18	100	<0.22
Nitenpyram	<0.18	<0.18	100
Fenhexamid	<0.18	NT <sup>b</sup>	NT
Tecloftalam	<0.18	NT	NT
Benalaxyl	<0.18	NT	NT
Acetamiprid	NT	<0.18	<0.22
Imidacloprid	NT	<0.18	<0.22
Dinotefuran	NT	119	<0.22
Thiacloprid	NT	0.21	<0.22
Thiamethoxam	NT	<0.18	<0.22

a. Each data is the mean of duplicates in independent examinations.

b. NT means not tested.

#### *Recovery of pesticides spiked in vegetables*

The recovery of the pesticides by the SPR immunosensor was examined using vegetable homogenates spiked with a mixture of boscalid, clothianidin, and nitenpyram. The lower quantitative limits of the three pesticides in vegetables were estimated to be 0.77 µg/g for boscalid, 0.34 µg/g for clothianidin, and 0.37 µg/g for nitenpyram from the preparation method of vegetable samples. The sensitivity was adequate to determine their concentrations around the MRLs for Welsh onion, lettuce, cucumber, tomato, broccoli, and spinach: 5 – 40 µg/g for boscalid, 1 – 40 µg/g for clothianidin, and 5 µg/g for nitenpyram. Mixtures of three pesticides were spiked at the following concentrations of boscalid, clothianidin, and nitenpyram: A) 2,

0.75, and 1.5  $\mu\text{g/g}$ ; B) 4, 1.5, and 3  $\mu\text{g/g}$ ; C) 8, 3, and 6  $\mu\text{g/g}$ . Table 3 shows that the recovery values were 75 – 90% for boscalid, 88 – 104% for clothianidin, and 72 – 105% for nitenpyram. The results suggested that the SPR immunosensor could determine the pesticides simultaneously with satisfactory recovery. The relative standard deviation (RSD) values associated with the recovery tests also showed a high repeatability at 0.00 – 10.1%, except for nitenpyram, which showed RSD values of 18.3% in Welsh onion (3  $\mu\text{g/g}$ ), 15.0% in spinach (3  $\mu\text{g/g}$ ), and 18.9% in spinach (6  $\mu\text{g/g}$ ). The results suggested that the constituted sensor is applicable for quantitative residue analysis of boscalid and clothianidin, and for the semi-quantitative analysis of nitenpyram in vegetables.

Table 3 Recovery examination of pesticide mixtures spiked in vegetables by the SPR immunosensor

Spiked pesticide conc. ( $\mu\text{g/g}$ )		Welsh onion		Lettuce		Cucumber		
		Rec <sup>a</sup>	RSD <sup>a</sup>	Rec	RSD	Rec	RSD	
A	Boscalid	2	79.7 <sup>b</sup>	2.49	76.4	1.44	77.2	0.00
	Clothidin	0.75	92.3	1.15	100	0.77	99.8	0.38
	Nitenpyram	1.5	78.0	8.63	80.8	5.07	84.1	6.91
B	Boscalid	4	87.2	2.49	78.9	1.44	89.6	2.49
	Clothidin	1.5	96.3	3.32	98.5	1.01	96.9	2.39
	Nitenpyram	3	84.1	18.3	98.5	5.07	95.2	6.91
C	Boscalid	8	83.8	3.80	85.5	1.44	88.8	1.44
	Clothidin	3	98.7	1.01	87.9	0.38	99.8	1.38
	Nitenpyram	6	90.7	1.91	94.1	1.92	101	5.07
Spiked pesticide conc. ( $\mu\text{g/g}$ )		Tomato		Broccoli		Spinach		
		Rec	RSD	Rec	RSD	Rec	RSD	
A	Boscalid	2	75.5	3.80	78.9	1.44	74.7	2.49
	Clothidin	0.75	96.7	3.66	97.4	1.92	95.6	2.39
	Nitenpyram	1.5	85.2	5.07	74.1	1.92	71.9	5.07
B	Boscalid	4	82.2	4.98	82.2	2.49	81.3	7.61
	Clothidin	1.5	94.5	2.99	99.6	1.33	98.7	4.32
	Nitenpyram	3	89.6	3.32	94.1	8.36	94.1	15.0
C	Boscalid	8	78.0	10.1	83.0	3.80	77.2	2.49
	Clothidin	3	100	2.39	104	1.15	95.8	1.53
	Nitenpyram	6	98.5	8.36	101	8.36	105	18.9

a. Rec shows recovery (%) and RSD shows relative standard deviation (%).

b. Each Rec. is the mean of triplicate in independent examinations.

### Correlation results between the dcELISA and the SPR immunosensor

The applicability of the SPR immunosensor was confirmed by comparing the results obtained from the immunosensor with those of the individual dcELISAs, which, except for nitenpyram, had been evaluated by previous studies.<sup>18,20</sup> As shown in Fig. 6, the SPR immunosensor results correlated highly with those of the dcELISAs:  $R^2 = 0.98$  for boscalid,  $R^2 = 1.00$  for clothianidin, and  $R^2 = 0.98$  for nitenpyram, with a slight bias of their slope: 0.77 for boscalid, 1.27 for clothianidin, and 1.12 for nitenpyram. It was confirmed that the developed SPR immunosensor could determine the three kinds of pesticides residues simultaneously in vegetables.

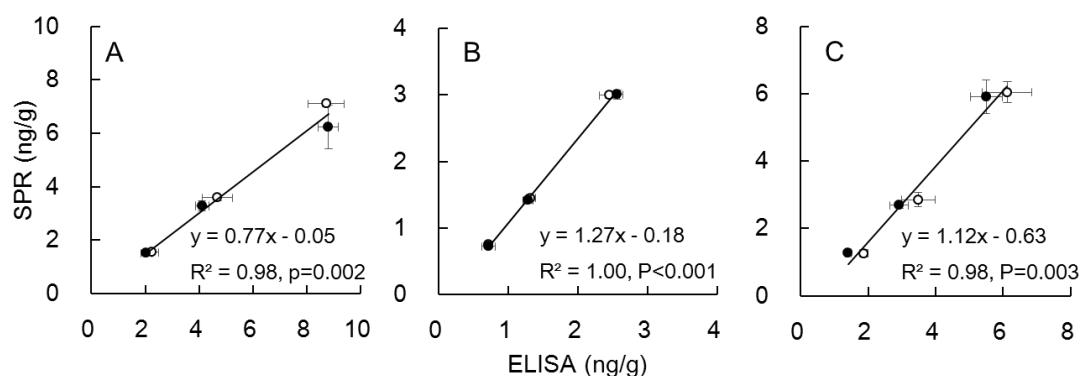


Fig. 6 Correlation of pesticide concentrations determined in cucumber (○) and tomato (●) samples spiked with mixture of 3 pesticides, between dcELISA and SPR-sensor: (A) boscalid, (B) clothianidin, and (C) nitenpyram. Each data point is the mean of triplicate in independent examinations; error bars indicate  $\pm$  SD.

### Conclusions

Our study indicated that the developed SPR immunosensor could be applied to the simultaneous analysis of the three pesticides: boscalid, clothianidin, and nitenpyram. The individual sensitivities were adequate to determine the concentrations around the MRLs of the

tested vegetables. The SPR immunosensor is applicable to a wide range of vegetables, such as Welsh onions, lettuce, cucumber, tomato, broccoli, and spinach, which belong to different families. The results also indicate that further development of simultaneous immunosensors is possible using the highly specific haptens and the high-affinity MoAbs. Such simultaneous SPR immunosensors would be useful for rapid, accurate, and simultaneous pesticide analyses.

## References

1. C. MacBean, “*The Pesticide Manual, In: Boscalid, 16th ed.*”, **2012**, British Crop Protection Council, Hampshire, 122.
2. C. MacBean, “*The Pesticide Manual, In: clothianidin, 16th ed.*”, **2012**, British Crop Protection Council, Hampshire, 225.
3. C. MacBean, “*The Pesticide Manual, In: nitenpyram, 16th ed.*”, **2012**, British Crop Protection Council, Hampshire, 809.
4. H. Uneme. Chemistry of clothianidin and related compounds. *J. Agric. Food Chem.*, **2011**, *59*, 2932.
5. X. Liu, F. Dong, D. Qin, and Y. Zheng. Residue analysis of kresoxim-methyl and boscalid in fruits, vegetables and soil using liquid-liquid extraction and gas chromatography-mass spectrometry. *Biomed. Chromatogr.*, **2010**, *24*, 367.
6. L. Lagunas-Allué, J. Sanz-Asensio, and M. T. Martínez-Soria. Comparison of four extraction methods for the determination of fungicide residues in grapes through gas chromatography-mass spectrometry. *J. Chromatogr. A*, **2012**, *1270*, 62.
7. A. Gulkowska, I. J. Buerge, and T. Poiger. Online solid phase extraction LC-MS/MS method for the analysis of succinate dehydrogenase inhibitor fungicides and its applicability to surface water samples. *Anal. Bioanal. Chem.*, **2014**, *406*, 6419.
8. A. Abad-Fuentes, E. Ceballos-Alcantarilla, J. V. Mercader, C. Agulló, A. Abad-Somovilla,

- and F. A. Esteve-Turrillas. Determination of succinate-dehydrogenase-inhibitor fungicide residues in fruits and vegetables by liquid chromatography-tandem mass spectrometry. *Anal. Bioanal. Chem.*, **2015**, *407*, 4207.
9. H. Obana, M. Okihashi, K. Akutsu, Y. Kitagawa, and S. Hori. Determination of acetamiprid, imidacloprid, and nitenpyram residues in vegetables and fruits by high-performance liquid chromatography with diode-array detection. *J. Agric. Food Chem.*, **2002**, *50*, 4464.
  10. H. Obana, M. Okihashi, K. Akutsu, Y. Kitagawa, and S. Hori. Determination of neonicotinoid pesticide residues in vegetables and fruits with solid phase extraction and liquid chromatography mass spectrometry. *J. Agric. Food Chem.*, **2003**, *51*, 2501.
  11. E. Watanabe, K. Baba, and H. Eun. Simultaneous determination of neonicotinoid insecticides in agricultural samples by solid-phase extraction cleanup and liquid chromatography equipped with diode-array detection. *J. Agric. Food Chem.*, **2007**, *55*, 3798.
  12. R. Hou, W. Jiao, X. Qian, X. Wang, Y. Xiao, and X. Xiao-Chun Wan. Effective extraction method for determination of neonicotinoid residues in tea. *J. Agric. Food Chem.*, **2013**, *61*, 12565.
  13. R. Raina-Fulton. Determination of neonicotinoid insecticides and strobilurin fungicides in particle phase atmospheric samples by liquid chromatography-tandem mass spectrometry. *J. Agric. Food Chem.*, **2015**, *63*, 5152.
  14. M. Gbylik-Sikorska, T. Sniegocki, and A. Posyniak. Determination of neonicotinoid insecticides and their metabolites in honey bee and honey by liquid chromatography tandem mass spectrometry. *J. Chromatogr. B*, **2015**, *990*, 132.
  15. Y. Akiyama, T. Matsuoka, N. Yoshioka, S. Akamatsu, and T. Mitsuhashi. Pesticide residues in domestic agricultural products monitored in Hyogo Prefecture, Japan, FY 1995–2009. *J.*

- Pest. Sci.*, **2011**, *36*, 66.
16. B. D. Morris and R. B. Schrinier. Development of an automated column solid-phase extraction cleanup of QuEChERS extracts, using a zirconia-based sorbent, for pesticide residue analyses by LC-MS/MS. *J. Agric. Food Chem.*, **2015**, *63*, 5107.
  17. A. David, C. Botías, A. Abdul-Sada, D. Goulson, and E. M. Hill. Sensitive determination of mixtures of neonicotinoid and fungicide residues in pollen and single bumblebees using a scaled down QuEChERS method for exposure assessment. *Anal. Bioanal. Chem.*, **2015**, *407*, 8151.
  18. M. Uchigashima, E. Watanabe, S. Ito, S. Iwasa, and S. Miyake. Development of immunoassay based on monoclonal antibody reacted with the neonicotinoid insecticides clothianidin and dinotefuran. *Sensors*, **2012**, *12*, 15858.
  19. E. Watanabe, S. Miyake, and Y. Yogo. Review of enzyme-linked immunosorbent assays (ELISAs) for analyses of neonicotinoid insecticides in agro-environments. *J. Agric. Food Chem.*, **2013**, *61*, 12459.
  20. Y. Hirakawa, T. Yamasaki, A. Harada, T. Ohtake, K. Adachi, S. Iwasa, N. Narita, and S. Miyake. Analysis of the fungicide boscalid in horticultural crops using an enzyme-linked immunosorbent assay and an immunosensor based on surface plasmon resonance. *J. Agric. Food Chem.*, **2015**, *63*, 8075.
  21. S. Miyake, Y. Ishii, Y. Yamaguchi, K. Ohde, M. Motoki, M. Kawata, S. Ito, Y. Yuasa, and H. Ohkawa, “*Environmental Fate and Effects of Pesticides*”, ed. J. R. Coats and H. Yamamoto, **2003**, 853, American Chemical Society, Washington, 124.
  22. M. Tomassetti, E. Martini, and L. Campanella. New immunosensors operating in organic phase (OPIEs) for analysis of triazinic pesticides in olive oil. *Electroanalysis*, **2012**, *24*, 842.
  23. R. Garcia-Febrero, E. Valera, A. Muriano, M. Pividori, F. Sanchez-Baeza, and M. Marco.

- An electrochemical magneto immunosensor (EMIS) for the determination of paraquat residues in potato samples. *Anal. Bioanal. Chem.*, **2013**, *405*, 7841.
24. C. March, J. Manclús, Y. Jiménez, A. Arnau, and A. Montoya. A piezoelectric immunosensor for the determination of pesticide residues and metabolites in fruit juices. *Talanta*, **2009**, *78*, 827.
  25. E. Mauriz, C. García-Fernández, J. Mercader, A. Abad-Fuentes, A. Escuela, and L. Lechuga. Direct surface plasmon resonance immunosensing of pyraclostrobin residues in untreated fruit juices. *Anal. Bioanal. Chem.*, **2012**, *404*, 2877.
  26. M. Tomassetti, E. Martini, L. Campanella, G. Favero, G. Sanzó, and F. Mazzei. A new surface plasmon resonance immunosensor for triazine pesticide determination in bovine milk: a comparison with conventional amperometric and screen-printed immunodevices. *Sensors*, **2015**, *15*, 10255.
  27. Y. Hirakawa, T. Yamasaki, E. Watanabe, F. Okazaki, Y. Murakami-Yamaguchi, M. Oda, S. Iwasa, H. Narita, and S. Miyake. Development of an immunosensor for determination of the fungicide chlorothalonil in vegetables, using surface plasmon resonance. *J. Agric. Food Chem.*, **2015**, *63*, 6325.
  28. S. Lu, X. Shao, Z. Li, Z. Xu, S. Zhao, Y. Wu, and X. Xu. Design, synthesis, and particular biological behaviors of chain-opening nitromethylene neonicotinoids with cis configuration. *J. Agric. Food Chem.*, **2012**, *60*, 322.
  29. H. Yamashita, M. Takai, M. Uchigashima, and S. Ito, Japan. Kokai Tokkyo Koho 2006, 2006282547 (in Japanese).
  30. S. Miyake, A. Hayashi, T. Kumeta, K. Kitajima, H. Kita, and H. Ohkawa. Effectiveness of polyclonal and monoclonal antibodies prepared for an immunoassay of the etofenprox insecticide. *Biosci. Biotechnol. Biochem.*, **1998**, *62*, 1001.

**Chapter 2      Development of a Surface Plasmon Resonance-Based  
Immunosensor for Detection of 10 Major O-antigens on Shiga  
Toxin Producing *Escherichia coli*, with Gel Displacement  
Technique to Remove Bound Bacteria**

**Abstract**

A surface plasmon resonance-based immunosensor (SPR-immunosensor) was developed for the detection of Shiga toxin-producing *Escherichia coli* (STEC) belonging to the O-antigen groups O26, O91, O103, O111, O115, O121, O128, O145, O157, and O159. The polyclonal antibodies (PoAbs) generated against each of the STEC O-antigen types in rabbits were purified and were immobilized on the sensor chip at 0.5 mg/mL. The limit of detection for STEC O157 by the SPR-immunosensor was found to be  $6.3 \times 10^4$  cells for 75 s. Each of the examined 10 O-antigens on the STECs was detected by the corresponding PoAb with almost no reaction to the other PoAbs. The detected STECs were sufficiently removed from the PoAbs using gelatin or agarose gel without deactivation of the PoAbs, enabling repeatable use of the sensor chip. The developed SPR-immunosensor can be applied for the detection of multiple STEC O-antigens. Furthermore, the new antigen removal technique using the gel displacement approach can be utilized with various immunosensors to improve the detection of pathogens in clinical and public health settings.

**Introduction**

Shiga toxin-producing *Escherichia coli* (STEC) is an intestinal bacterium that infects humans who consume contaminated foods and drinks. STEC pervades widely through the food chain across a broad geographical area at low temperatures, resulting in a high number of infections annually. Patients infected with STEC often progress to hemorrhagic colitis and

hemolytic uremic syndrome because of delayed treatment, sometimes resulting in kidney failure or death.<sup>1</sup> Rapid detection of the pathogen is important for treating such patients. Serotyping of the bacterial O-antigens is generally used to detect STEC infection.<sup>2</sup> Serotyping has been carried out using the agglutination reaction between the pathogens and antisera, but it is difficult to digitalize the observation. PCR is also used for serotyping, but it is time-consuming and labor-intensive. Thus, an alternative detection method with a greater reliability and shorter detection time is required for use in clinical and public health settings.

While O157 is the major STEC O-antigen among about 180 different O-antigen types, many other O-antigens have been isolated from contaminated patients, foods, and drinks.<sup>3</sup> The following O-antigen types accounted for 53% of the O-antigens detected between 2000 and 2012 in Japan: O26 (35%), O111 (8%), O103 (4%), O121 (3%), O145 (2%), and others (1%).<sup>4</sup> A method for detecting O157 and the five other most common O-antigens in foods was announced by the Ministry of Health, Labour, and Welfare in Japan in 2014. Additionally, in the USA, non-O157 O-antigens accounted for 51% of STEC infections in 2012 according to the Foodborne Diseases Active Surveillance Network.<sup>5</sup> Approaches for regulating O26, O45, O103, O111, O121, O145, and O157 in raw beef were announced by the USDA in 2012.<sup>6</sup> In addition to these O-antigens, more than 90 other O-antigen types have been isolated from patients.<sup>7-14</sup> Therefore, a method for the simultaneous detection of multiple O-antigens on STECs would be useful in clinical and public health settings.

Immunosensors have attracted attention as automatic and reliable detection methods for *E. coli* O157. Various electrochemical immunosensors were successfully developed for the detection of *E. coli* O157 using indium tin oxide, interdigitated array, screen-printed carbon, and gold electrodes.<sup>15-18</sup> A piezoelectric immunosensor was developed using a quartz crystal microbalance.<sup>19</sup> Surface plasmon resonance-based immunosensors (SPR-immunosensors) have also been developed by utilizing an anti-*E. coli* O157:H7 antibody immobilized to a thin gold

film surface on a glass prism.<sup>20,21</sup> An SPR-immunosensor was reported to be highly sensitive for detecting *E. coli* O157 (the reported sensitivity was 2.8 colony-forming units [cfu]/mL) combined with the on-chip culture technique.<sup>22</sup> For the detection of multiple bacterial antigens, an SPR-immunosensor was developed to detect a maximum of 4 of the following bacteria using micro-channels: *E. coli* O157, *Salmonella choleraesuis*, *Listeria monocytogenes*, and *Campylobacter jejuni*.<sup>23</sup> Another SPR-immunosensor designed as a batch system, in which the sensor chip is sterilized with a diluted bleach solution after each use, was developed to detect 7 O-antigens on STECs.<sup>24</sup> However, multi-detection methods for O-antigens on STECs that allow for the continuous loading of a series of contaminated samples have not been reported, although there is a need for this technology. This may be because of difficulties in removing bacterial cells bound to the immobilized antibody on the sensor surface without deactivating the antibody. Alternative methods that do not involve antibodies have been proposed, including using bacteriophages, lectins, and carbohydrates.<sup>25-27</sup> However, it is difficult to achieve both multiple and specific detection of STEC O-antigens using these methods.

In this study, we developed a reliable multi-detection method for major STEC O-antigens by continuously loading a series of contaminated samples using an SPR-immunosensor with a microarray-type sensor chip, on which 10 types of polyclonal antibodies (PoAbs) corresponding to individual STEC O-antigens were immobilized. Furthermore, we developed a versatile method for removing a wide range of pathogenic bacterial cells bound to the antibodies without deactivating the antibodies with a new “displacement” technique using a gel. This is the first report of a reliable multi-detection method for bacterial antigens by continuously loading samples, including major STEC O-antigens, using an immunosensor and a sensor chip that can be reused.

## **Experimental**

### *Materials*

Rabbit antisera specific to each of the *E. coli* O-antigens O26, O91, O103, O111, O115, O121, O128, O145, O157, and O159 were purchased from Denka Seiken Co., Ltd. (Tokyo, Japan). For the preparation of the sera by Denka Seiken Co., Ltd., each rabbit was immunized with the corresponding bacterial cells inactivated by formaldehyde, cross reactive PoAbs were removed from the sera using an absorption technique using inactivated *E. coli* of various O-antigen types, and the specified antisera were adjusted to the same titer after an agglutination test.<sup>28</sup> Protein G beads (Sepharose 4 Fast Flow) were purchased from GE Healthcare (Little Chalfont, UK). The polyvinylidene difluoride membrane (0.2  $\mu$ m) was purchased from Atto Co. (Tokyo, Japan). Horseradish-peroxidase (HRP)-labeled goat anti-rabbit immunoglobulin (IgG) (H+L) antibody was purchased from Abcam plc. (Cambridge, UK). The chemiluminescent substrate of HRP for western blot analysis was purchased from Thermo Fisher Scientific (Waltham, MA, USA). Rabbit anti-mouse IgG PoAb was purchased from Dako (Glostrup, Denmark). Bovine serum albumin (BSA) was purchased from Sigma-Aldrich Co. (St. Louis, MO, USA). Gelatin, agarose, and all other chemicals and reagents of analytical grade were purchased from Nacalai Tesque (Kyoto, Japan).

#### *STEC isolates*

STEC strains isolated from patients used in this study are listed in Table 1. They were collected by the Kobe Institute of Health (Kobe, Japan), and the species were identified by the conventional indole test, methyl red test, Voges–Proskauer test, and citrate test. The O-antigen serotype was confirmed by the conventional agglutination test with rabbit antisera against each of the STEC O-antigens.<sup>2</sup> The presence of the Shiga toxin gene was confirmed by conventional PCR.<sup>29</sup> The STEC strains were cultured overnight at 35°C on LB agar plates or in 2 mL of LB medium. Bacterial colonies produced on the plate were suspended in the running buffer of the SPR-immunosensor described below, and the suspension was immediately examined using the

sensor. The cultured bacterial cells in LB medium were directly used for examination. The bacterial cell numbers were counted as cfu after incubation on LB agar plates overnight at 35°C or by measuring optical density at 530 nm using a Vi-spec 2 turbidimeter (Kyokuto Pharmaceutical Industrial Co., Ltd, Tokyo, Japan). The colonies were alternatively resuspended in 0.2% formaldehyde overnight at 4°C and subsequently heated for 20 min at 80°C to fix the bacterial cells. The fixed cells were then used for western blot analysis.

Table 1 STEC strains isolated from patients

<b>Serotype</b>	<b><i>stx</i><sub>1</sub></b>	<b><i>stx</i><sub>2</sub></b>
<b>O26</b>	+	+
<b>O91</b>	+	–
<b>O103</b>	+	–
<b>O111</b>	+	–
<b>O115</b>	+	–
<b>O121</b>	–	+
<b>O128</b>	+	+
<b>O145</b>	+	–
<b>O157</b>	+	+
<b>O159</b>	+	+

*Preparation of O-antigen specific PoAbs*

Anti-O-antigen PoAbs were purified from rabbit antisera to the STEC O-antigens (O26, O91, O103, O111, O115, O121, O128, O145, O157, and O159) using Protein G beads. Each 100 µL of beads was suspended in 100 µL of phosphate-buffered saline (PBS; 10 mM phosphate, 150 mM NaCl; pH 7.0), and then added to 1 mL of antisera. The mixture was gently stirred overnight at 4°C. After the beads were washed 3 times with 1 mL of PBS, the supernatant was removed by centrifugation at 9393 × g for 1 min. The PoAbs bound to the beads were eluted with 100 µL of

100 mM citrate solution (pH 2.5). The eluted PoAb solution was immediately neutralized with 15  $\mu$ L of 1.0 M trisodium phosphate and used for SPR-immunosensor constitution. The prepared PoAbs were abbreviated as anti-O26, anti-O91, anti-O103, anti-O111, anti-O115, anti-O121, anti-O128, anti-O145, anti-O157, and anti-O159. The protein concentration of each PoAb was determined by a protein assay using Coomassie brilliant blue solution (Nacalai Tesque) according to the manufacturer's instruction manual.

#### *Western blot analysis*

Fixed cells of STEC O26, O91, O103, O111, O115, O121, O128, O145, O157, and O159 ( $1.0 \times 10^7$  cells) were suspended in 20  $\mu$ L of sample buffer (62.5 mM Tris-HCl, pH 7.0 modified with 1% sodium dodecyl sulfate (SDS), 0.01% bromophenol blue, and 10% glycerol), and then incubated for 15 min at 25°C to lyse the cells. After centrifugation at  $9393 \times g$  for 10 min, the supernatant was boiled for 5 min and separated by SDS-polyacrylamide gel electrophoresis with a 15% polyacrylamide running gel. The O-antigens were blotted onto the polyvinylidene difluoride membrane using a semi-dry blotter (NA-1512; Nihon Eido Co. Ltd., Japan) at 0.5 mA/cm<sup>2</sup> for 2.5 h in transfer buffer (62.5 mM Tris base, 200 mM glycine, and 20% ethanol). The membrane was blocked with PBS containing 0.1% Tween<sup>®</sup> 20 (PBS-T) containing 5% skim milk at 4°C overnight, and then washed once with PBS-T. Membranes were transferred to anti-O26, anti-O111, or anti-O157 PoAb (each 1.0  $\mu$ g/mL) solution in PBS-T containing 0.3% skim milk, and then incubated at 25°C for 1 h. After washing 4 times with PBS-T, the membrane was further incubated with HRP-labeled anti-rabbit IgG antibody (0.5  $\mu$ g/mL) in PBS-T containing 0.3% skim milk at 25°C for 1 h. After washing 4 times with PBS-T, the antigen bands formed from reaction with the anti-O-antigen PoAbs were developed using the chemiluminescent substrate of HRP according to the manufacturer's instruction manual. The band on the membrane was detected using a gel imager (ImageQuant<sup>™</sup> LAS 4000; GE Healthcare).

### *SPR-immunosensor*

The surface plasmon resonance imaging system was purchased from HORIBA Scientific (OpenPlex; Palaiseau, France). The biochip consisted of a prism and a gold thin-layer, the surface of which was modified with molecules terminated in a carboxyl group (SPRi-Biochip CS-HD, HORIBA Scientific). Since the carboxyl groups were pre-activated by esterification with *N*-hydroxysuccinimide, the target antibodies could bind directly to the biochip.

#### *1) Preparation of sensor chip*

Purified anti-O-antigen PoAbs and anti-mouse IgG PoAb (control) were diluted in PBS (0.10–0.75 mg/mL). To immobilize the PoAb on the chip by covalent bonding, these PoAb solutions were respectively spotted onto the chip surface at 10 nL/spot using a spotter (Spot Master; Musashi Engineering, Tokyo, Japan) in 80% relative humidity. The spotted sensor chip was incubated at 4°C for 16 h in 80% relative humidity. The chip surface was then washed 3 times with PBS. The surface was blocked with PBS containing 1% BSA at 25°C for 30 min and washed 3 times with PBS. Unreacted carboxyl groups were deactivated with 1 M ethanolamine solution (pH 8.5) at 25°C for 30 min, and then washed 3 times with PBS. The prepared sensor chip was set into the instrument according to the manufacturer's instruction manual. The reaction chamber for detecting STEC O-antigens was composed of a flow cell (volume ~ 80 µL) attached to the sensor chip surface through a hexagonal gasket.

#### *2) Flow conditions for the reaction*

All reactions were carried out at 25°C. Running buffer (PBS containing with 0.2% BSA and 0.02% Tween® 20) was degassed using a degasser (DEGASi® Classic; Biotech, Onsala, Sweden), and was set up to continuously flow into the reaction chamber, driven by a peristaltic pump (MINIPULS® 3; Gilson, Inc., Middleton, WI, USA) at 50 µL/min. The prepared bacterial cell suspension was preserved in a sample loop (volume = 200 µL) and was set up to flow into

the chamber when the valve was switched to the injection mode.

### *3) Detection of STEC O-antigens*

The sensor chip was irradiated by a light-emitting diode ( $\lambda = 810$  nm) and the light was reflected at the interface between the prism and the gold thin layer with attenuation by SPR phenomena. The intensity of the reflected light (reflectivity) was acquired by an 8-bit charge-coupled device (CCD) camera every 3 s. After 200  $\mu$ L of the bacterial cell suspension was injected, the reflectivity of each spot changed depending on the quantity of the bacterial cell bound to the PoAbs. The percent change of the reflectivity ( $\% \Delta R$ ) every 3 s was calculated based on the CCD signal, and was averaged within a pre-defined detection area on each spot of the PoAbs. The data for each test antibody were normalized by subtracting the reflectivity for anti-mouse IgG PoAb. The  $\% \Delta R$  was visualized as a bright spot that could easily be distinguished from the background by the CCD camera.

### *4) Regeneration of the sensor chip*

Gelatin (3.0 g) was dissolved with 100 mL of distilled water at 80°C, and was gelled by cooling at 4°C for 7 days. Agarose (0.2 g) was dissolved with 100 mL of boiled distilled water, and was gelled by cooling at 25°C for 1 h. After the detection of each O-antigen, 50  $\mu$ L of 10 mM NaOH, 100 mM glycine buffer (pH 2.0), or the above gel suspension (3% gelatin gel kept on ice immediately before use or 0.2% agarose gel) was set to flow into the reaction chamber for 1 min at 50  $\mu$ L/min. The residual gel was flushed out from the chamber with running buffer at 1 mL/min. The efficiency of removal of the bound cells was confirmed by monitoring the SPR signals. The sensor chip was reused for the next detection of the STEC O-antigens without any other treatments after the signals had sufficiently returned to baseline.

## **Results and Discussion**

### *Reactivity of anti-O-antigen PoAbs*

The anti-O26, anti-O111, and anti-O157 PoAbs were examined to confirm that they specifically reacted with each corresponding O-antigen on STEC by western blot analysis, as shown in Fig. 1. When the blotted membrane was reacted with anti-O26 PoAb, a characteristic ladder band of the O-antigen was located at 14–28 kDa and 48–64 kDa in the O26 antigen lane as shown in Fig. 1A. In the reaction with anti-O111 PoAb, a band was located at 32–90 kDa in the O111 antigen lane, as shown in Fig. 1B. In the reaction with anti-O157 PoAb, a band was located at 42–87 kDa of the O157 antigen lane, as shown in Fig. 1C. Characteristic ladder bands are produced by repeat oligosaccharide structures containing 2–7 sugar residues. The bands reacted with anti-O26, anti-O111, and anti-O157 PoAbs and showed the same patterns as observed in previous studies.<sup>30,31</sup> We confirmed that the 3 PoAbs examined specifically reacted with their corresponding O-antigens. The other PoAbs were also specific for their corresponding O-antigens (data not shown).

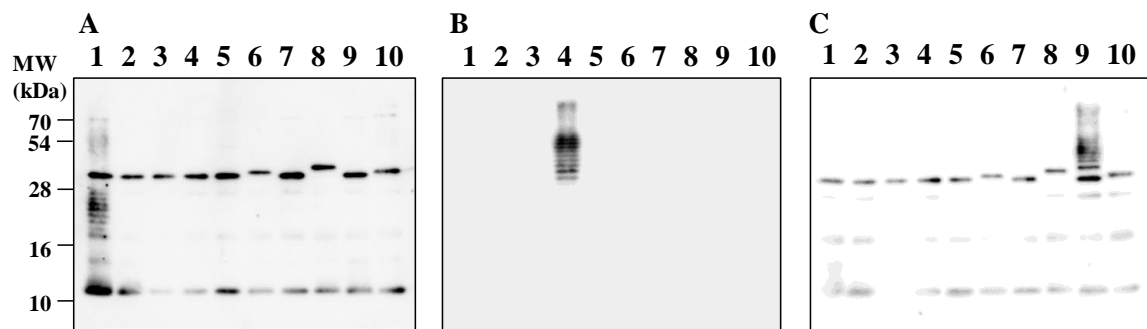


Fig. 1 Reactivity of prepared PoAbs with 10 O-antigens on STECs by western blot analysis. Results of reactivity with A) PoAb O26, B) PoAb O111, and C) PoAb O157 are shown. Lanes 1–10 show the O26, O91, O103, O111, O115, O121, O128, O145, O157, and O159 antigens, respectively.

Anti-O111 PoAb did not react with common antigens in the STECs examined. However,

anti-O26 and anti-O157 PoAbs reacted with common antigens, including 11, 18, and 37 kDa proteins. These results are as would be expected, given that the examined PoAbs were prepared using inactivated whole bacteria cells.<sup>28</sup> However, these proteins are not present on the surface of bacterial cells and differ from the O-antigens. Thus, the reactivity of the PoAbs with common antigens may have only a negligible influence on the direct detection of O-antigen in viable cells. All of the prepared PoAbs were used for SPR-immunosensor constitution.

#### *Immobilization of PoAbs to the sensor chip surface*

Immobilization of anti-O157 PoAb was examined. The PoAb solution was serially diluted with PBS to 0.10, 0.25, 0.50, and 0.75 mg/mL and then spotted onto the sensor chip surface containing carboxylic acid pre-activated with *N*-hydroxysuccinimide. The amino groups on lysine residues of the PoAb were covalently bound without treatment. The PoAb-immobilized chip was placed in the SPR-immunosensor and STEC O157 cells suspended in running buffer were injected at  $10^7$  cfu/mL. The reaction signal (% $\Delta$ R) increased in a time-dependent manner and reached a plateau (0.7) by 300 s at more than 0.5 mg/mL of PoAb concentration, as shown in Fig. 2. We assumed that lysine residues immobilized with carboxylic acid would be present in the same numbers in the constant region of all PoAbs. A concentration 0.5 mg/mL was used to immobilize the PoAbs.

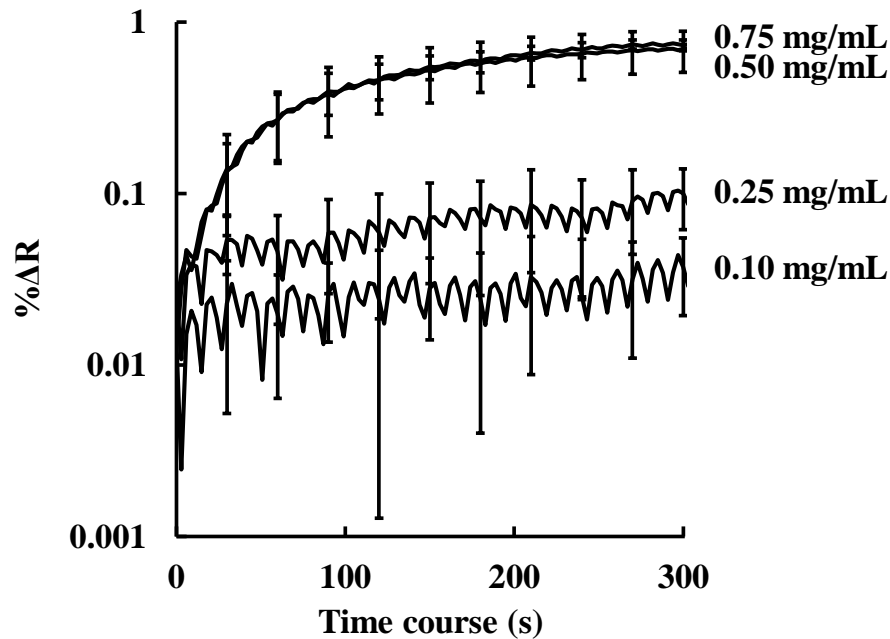


Fig. 2 Time-course of the reaction between each concentration of anti-O157 PoAbs and  $10^7$  cfu/mL of STEC O157 cells as quantified using the SPR-immunosensor. The PoAb concentrations are described on the right of each reaction curve. The error bars indicate the standard deviation of 4 independent experiments.

#### *Sensitivity of constituted SPR-immunosensor*

To determine the sensitivity of the constituted SPR-immunosensor, STEC O157 cells were suspended in running buffer at  $10^5$ ,  $10^6$ ,  $10^7$ , and  $10^8$  cfu/mL. The cell suspensions were respectively injected into the SPR-immunosensor. The % $\Delta$ R values at 300 s were  $0.012 \pm 0.008\%$  at  $10^5$  cfu/mL,  $0.08 \pm 0.01\%$  at  $10^6$  cfu/mL,  $0.69 \pm 0.09\%$  at  $10^7$  cfu/mL, and  $6.5 \pm 0.5\%$  at  $10^8$  cfu/mL (Fig. 3). The minimum time to obtain quantitative results at 3 folds standard deviation (3SD) from the control value was 75 s at  $10^6$  cfu/mL. Because the flow rate was 50  $\mu$ L/min, the minimum number of cells required for analysis was  $6.3 \times 10^4$  cells. This cell number was defined based on the limit of detection for O-157 on STEC cells.

The SPR-immunosensor showed sufficient sensitivity and rapidity for detecting O-antigens

on STEC cells from colonies on agar plates or from culture fluids containing STEC cells. However, the sensitivity would be higher when examining contaminated foods and drinks.

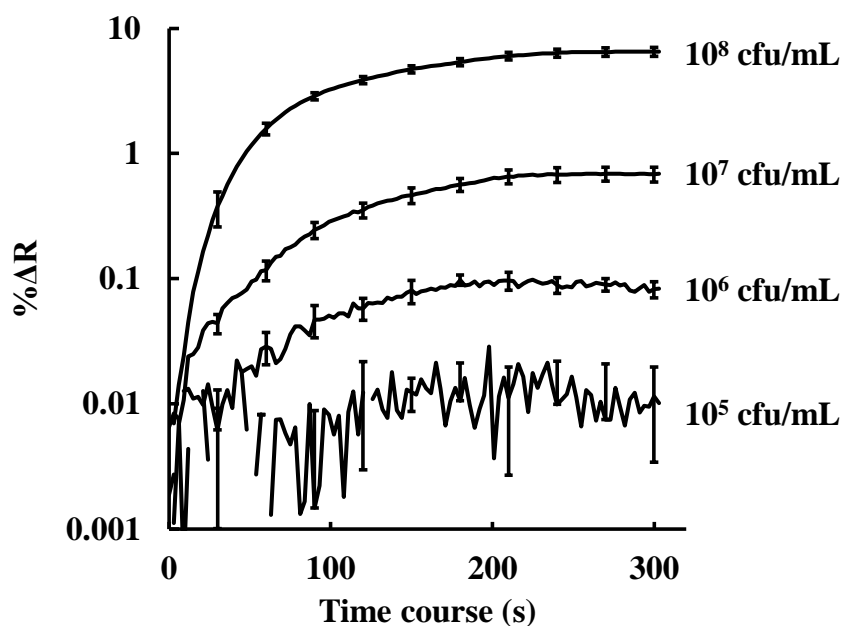


Fig. 3 Time-course of the reaction between 0.5 mg/mL of anti-O157 PoAb and each cell number of STEC O157 as quantified using the SPR-immunosensor. The cell numbers are described on the right of each reaction curve. The error bars indicate the standard deviation of 3 independent experiments.

#### *Removal of STEC cells bound on sensor-chip surface*

The removal of STEC cells bound to PoAbs on the sensor chip was examined as an approach to enable the repeated detection of O-antigens using the SPR-immunosensor. The 10 purified PoAbs against the O-antigens of STEC were covalently immobilized on the chip as individual spots. Additionally, a mixture of the 10 STECs listed in Table 1 was suspended in running buffer at  $10^7$  cfu/mL. After injection into the sensor, all reaction signals increased in a time-dependent manner and antigen-antibody complexes formed (Fig. 4). After the buffer was

changed to running buffer, the % $\Delta$ R was stabilized at 0.9% for O26, 0.3% for O91, 0.6% for O103, 1.1% for O111, 0.5% for O115, 0.8% for O121, 0.5% for O128, 0.7% for O145, 0.7% for O157, and 0.8% for O159. The signal strength varied between 0.3–1.1%, even though the antibody and the bacteria were essentially applied at the same concentrations. This result seemed to derive from the differences in the antibody titer and/or the antigen density on the bacteria cells. Differences in the antibody titer can occur owing to the differences in responsiveness among different individual immunized rabbits. The antigen density on bacterial cells might also vary among the different STEC strains. We plan to clarify the reasons for these observations further by performing future examinations using various STEC isolates.

The % $\Delta$ R induced by the STEC cells injection showed little or no change resulting from the inflow of the running buffer. The STEC cells were rigidly bound to the immobilized PoAbs at multiple epitopes. When the bound antigens were low-molecular weight compounds such as pesticides, the signals were gradually decreased by the dissociation of the antigen-antibody complex during the inflow of running buffer, and the removal of the antigens was not difficult.<sup>32,33</sup> Thus, removing STEC cells may be more difficult than removing low-molecular weight compounds.

The most widely used method for removing bacteria is the use of diluted NaOH.<sup>20,21,34,35</sup> This approach was initially examined as shown in Fig. 4A. After the injection of 10 mM NaOH solution, the % $\Delta$ R did not return to the baseline, except for that of O115. Furthermore, the signals for O26, O91, and O121 decreased to below the baseline value. In these cases, the PoAbs may have been partially denatured. As an alternative, 100 mM glycine buffer (pH 2.0), which is generally used as the dissociation buffer in various SPR-immunosensors,<sup>36-39</sup> was examined. The results showed that it was quite difficult to remove the bound STECs from the immobilized PoAbs (Fig. 4B). Dilute NaOH (alkali) and glycine buffer (acid) can dissociate the antigen-antibody complex by disrupting hydrogen bonds and/or ionic bonds. The O-antigens were composed of

polysaccharides, and hydrogen bonding is thought to be a major factor in their binding. However, the chemical conditions described above were too weak to dissociate the bound STECs. Thus, dissociation was not achieved using these commonly reported methods.

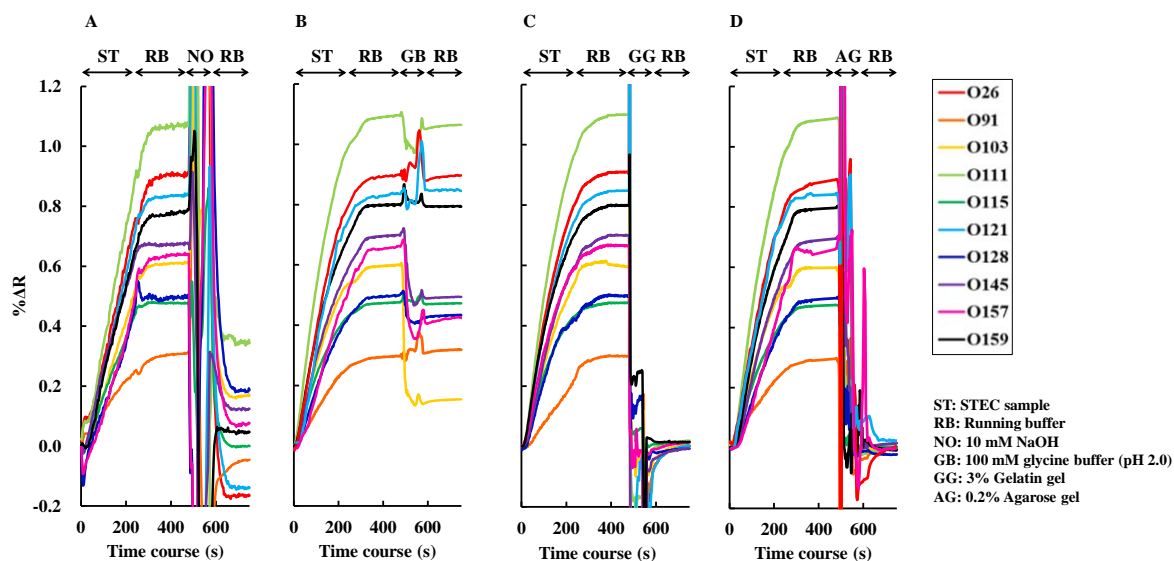


Fig. 4 Time-courses of the reaction between each of the PoAbs and a mixture of the STECs presenting each of the 10 O-antigens (each  $10^7$  cfu/mL) and of the removal of bound STECs after the injection of the following reagents, as quantified using the SPR-immunosensor. A) 10 mM NaOH, B) 100 mM glycine buffer (pH 2.0), C) 3% gelatin gel, and D) 0.2% agarose gel. The names of the PoAbs that reacted are described in the right column.

We examined whether physical conditions, such as displacement by gelatin or agarose gels, could disrupt only the hydrogen bonds between O-antigens and PoAbs, but not the covalent bonds between PoAbs and carboxyl groups on the sensor chip. The gelatin gel and agarose gel were respectively adjusted to 3% and 0.2% to maintain a semisolid condition that could be easily injected into the SPR-immunosensor. The 3% gelatin gel was cooled on ice immediately before use to prevent melting. When both gels were used, each % $\Delta$ R returned to the baseline value as

shown in Fig. 4C and 4D. When the anti-O157 PoAb immobilized spot, on which STEC O157 cells were bound, was observed under a dark field microscope, numerous cells were found on the spot as shown in Fig. 5A and 5C. The number of cells was drastically lower after displacement by a 3% gelatin gel as shown in Fig. 5D and 5F. The number of residual cells was approximately the same as the number of non-specifically bound cells observed for the negative control as shown in Fig. 5B and 5E. These signals returned to their respective baseline values after displacement of the cells in the gelatin and agarose gels. The other serotypes yielded highly similar results (data not shown).

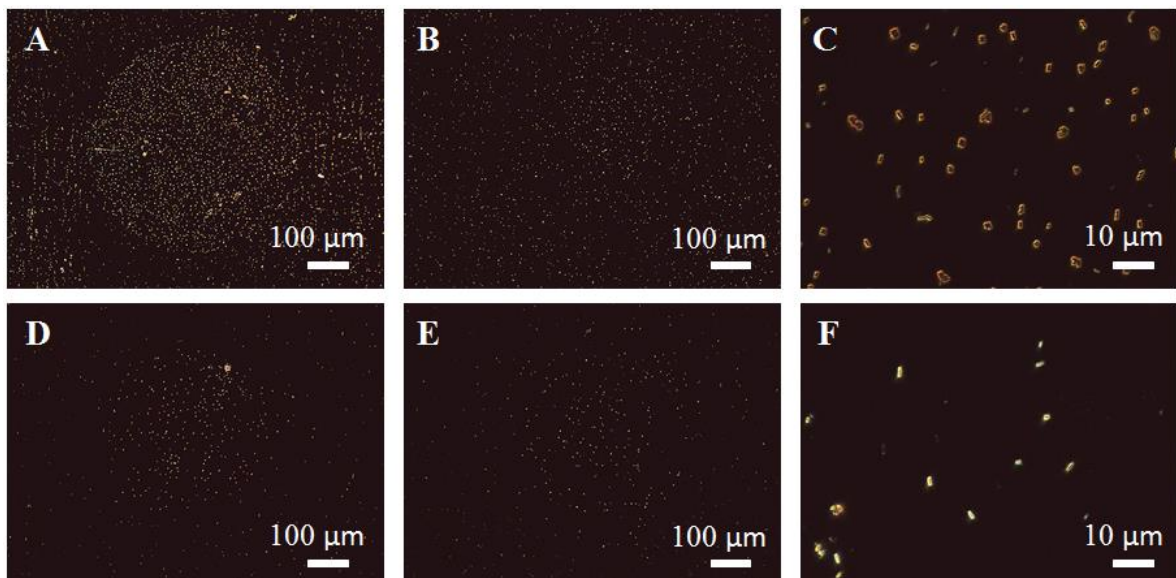


Fig. 5 Typical spot image observed under a dark field microscope (BX51M: Olympus Co., Tokyo, Japan). STEC O157: A) bound to the anti-O157 PoAb ( $\times 10$ ), B) bound to the anti-mouse IgG PoAb (negative control;  $\times 10$ ), and C) bound to the anti-O157 PoAb ( $\times 100$ ). STEC O157 after displacement by 3% gelatin: D) bound to the anti-O157 PoAb ( $\times 10$ ), E) bound to the anti-mouse IgG PoAb (negative control;  $\times 10$ ), and F) bound to the anti-O157 PoAb ( $\times 100$ ).

The gel displacement approach effectively disrupted the hydrogen bonds between the O-antigens and the PoAbs and removed the STECs from the PoAbs. The sensor chip regenerated

using the gels was repeatedly used without any loss of the binding ability of the immobilized PoAbs. Therefore, the gels were not sufficiently strong to remove PoAbs immobilized on the sensor chip by covalent bonds. In addition, the gels could physically displace the bacteria, while the PoAbs are too small to be removed by the gels. These size differences would also allow effective selective removal. The 3% gelatin gel was particularly suitable for repeated use because it could be easily removed from the sensor chip surface, whereas the 0.2% agarose gel was more difficult to remove. This displacement technique could potentially be widely used for removing other various antigen-antibody complexes, such as other bacteria, viruses, and fungi.

#### *Detection of various STEC O-antigens by SPR-immunosensor*

Each colony of the 10 STECs was suspended in running buffer and adjusted to an optical density of 0.5–1.0 (530 nm). These optical density measurements indicate a bacterial number of  $10^7$ – $10^8$  cfu/mL. Each of the bacterial suspensions was injected into the SPR-immunosensor, onto which each of the 10 PoAbs was spotted as shown in Fig. 6A. The signal image was developed in real-time as a sharp outline and bright spot, such as the image of STEC O157 (Fig. 6B). The highest  $\% \Delta R$  signal always developed with the corresponding PoAb among the 10 PoAbs (Fig. 7). The constituted SPR-immunosensor specifically detected each serotype of the STEC O-antigens from the colony among the examined 10 STECs, although STEC O26 also weakly bound with anti-O159 PoAb.

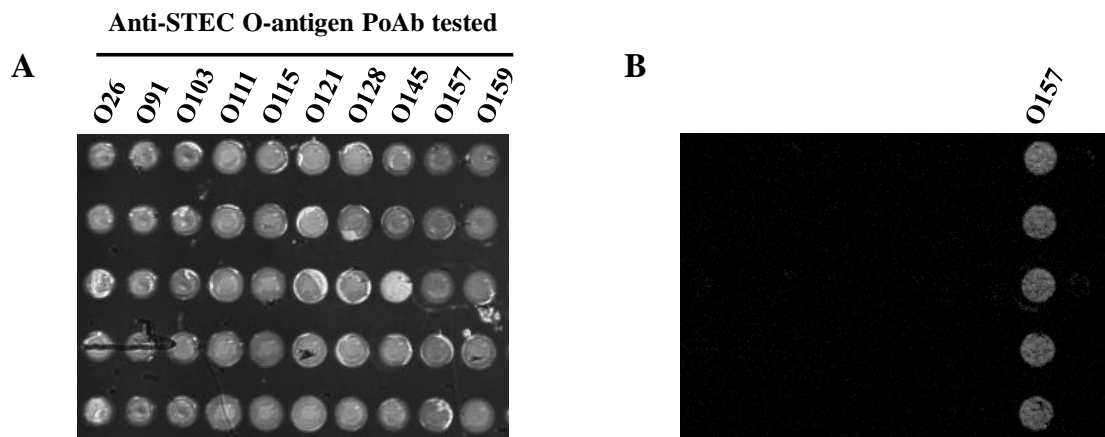


Fig. 6 A) Raw optical images of each spot on which the anti-O-antigen PoAbs were immobilized on the chip. B) Bright spot image of the differential  $\% \Delta R$  after reaction with STEC O157.

STECs were also cultured overnight at 30°C in LB broth. The bacterial fluids were directly injected into the SPR-immunosensor, and the O-antigens were detected for all STEC samples as well as the above colonies; however, it was difficult to monitor the signal in real-time because of the differences in composition between the medium and the running buffer (data not shown). Other liquid samples were also successfully applied, such as mEC medium (0.5% NaCl, pH 6.9), which is commonly used in STEC culture, as well as vegetable juice and milk (data not shown).

Anti-O159 PoAb showed weak binding to STEC O26 as well as strong binding to STEC O159, as shown in Fig. 7. STEC O26 was sufficiently dissociated by the injection of 100 mM glycine buffer (pH 2.0) for 30 s without applying the gel displacement method. The polysaccharide of the O26 antigen contains trisaccharide repeating units without side chains, but the O159 antigen contains tetrasaccharide repeating units each having 1 side chain. Both structures contain  $\alpha$ -L-Fuc-(1-3)- $\beta$ -D-GlcNAc-(1-), but the Fuc of the O26 is *N*-acetylated in O159.<sup>40</sup> These similar features or other common structural elements may have resulted in a cross-reaction. The results indicate that STEC O26 bound to anti-O159 PoAb through weaker hydrogen

bonds than those involved in STEC O159 binding to the antibody, and the glycine buffer removal method dissociated the bonds.

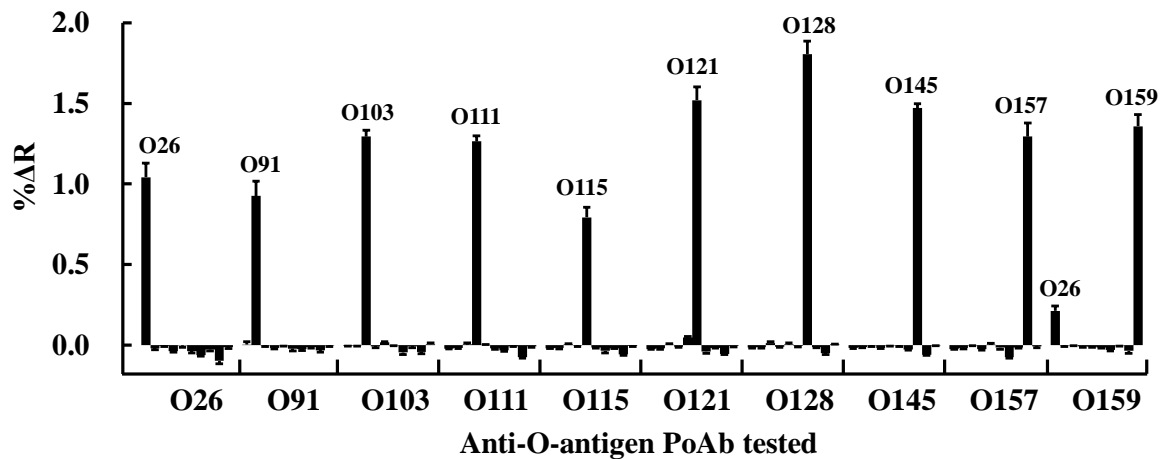


Fig. 7 Reactivity of each of the immobilized PoAbs with the O-antigens on STECs (injected at  $10^7$  cfu/mL). The STEC O-antigen for which the strongest reaction was observed is described in the graph. The error bars indicate the standard deviation of 5 independent experiments.

## Conclusions

A reliable multiple analyte SPR-immunosensor was developed using 10 PoAbs. The SPR-immunosensor was used to identify 10 STEC O-antigens in a single test. The sensor chip used in this study can be used to immobilize up to 400 different antibodies. In theory, it should be possible to identify all 180 known STEC O-antigens in a single test. Furthermore, the newly developed gel displacement technique withstood repeated use of the sensor chip for the detection of multiple bacteria cell samples, which has been difficult to achieve in the past. Such SPR-immunosensors using this gel displacement technique will contribute to the multi-detection not only of STECs, but also of other important pathogens in clinical and public health settings.

## References

1. L. B. Robert, and P. D. Michael. Foodborne Disease Significance of *Escherichia coli* O157:H7 and Other Enterohemorrhagic *E. coli*. *Food Technology Magazine*, **1997**, *51*, 69.
2. I. Ørskov, F. Ørskov, B. Jann, and K. Jann. Serology, chemistry, and genetics of O and K antigens of *Escherichia coli*. *Bacteriol. Rev.*, **1977**, *41*, 667.
3. E. Scallan, R. M. Hoekstra, F. J. Angulo, R.V. Tauxe, M. A. Widdowson, S. L. Roy, J. L. Jones, and P. M. Griffin. Foodborne illness acquired in the United States—major pathogens. *Emerg. Infect. Dis.*, **2011**, *17*, 7.
4. J. Terajima, S. Iyoda, M. Ohnishi, and H. Watanabe. Shiga toxin (verotoxin)-producing *Escherichia coli* in Japan. *Microbiol. Spectr.*, **2014**, *2*.
5. Centers for Disease Control and Prevention. Incidence and trends of infection with pathogens transmitted commonly through food—foodborne diseases active surveillance network, 10 U.S. sites, 1996-2012. *MMWR.*, **2013**, *62*, 283.
6. Food Safety and Inspection Service, USDA. Rules and regulations. *Federal Register*, **2012**, *77*, 31975.
7. J. E. Blanco, M. Blanco, M. P. Alonso, A. Mora, G. Dahbi, M. A. Coira, and J. Blanco. Serotypes, virulence genes, and intimin types of Shiga toxin (verotoxin)-producing *Escherichia coli* isolates from human patients: prevalence in Lugo, Spain, from 1992 through 1999. *J. Clin. Microbiol.*, **2004**, *42*, 311.
8. J. T. Brooks, E. G. Sowers, J. G. Wells, K. D. Greene, P. M. Griffin, R. M. Hoekstra, and N. A. Strockbine. Non-O157 Shiga toxin-producing *Escherichia coli* infections in the United States, 1983-2002. *J. Infect. Dis.*, **2005**, *192*, 1422.
9. Y. T. van Duynhoven, I. H. Friesema, T. Schuurman, A. Roovers, A. A. van Zwet, L. J. Sabbe, W. K. van der Zwaluw, D. W. Notermans, B. Mulder, E. J. van Hannen, F. G. Heilmann, A. Buiting, R. Jansen, and A. M. Kooistra-Smid. Prevalence, characterisation and clinical profiles of Shiga toxin-producing *Escherichia coli* in The Netherlands. *Clin. Microbiol.*

*Infect.*, **2008**, *14*, 437.

10. M. M. Aslani, and S. Bouzari. Characterization of virulence genes of non-O157 Shiga toxin-producing *Escherichia coli* isolates from two provinces of Iran. *Jpn. J. Infect. Dis.*, **2009**, *62*, 16.
11. E. B. Hedican, C. Medus, J. M. Besser, B. A. Juni, B. Koziol, C. Taylor, and K. E. Smith. Characteristics of O157 versus non-O157 Shiga toxin-producing *Escherichia coli* infections in Minnesota, 2000-2006. *Clin. Infect. Dis.*, **2009**, *49*, 358.
12. M. R. Couturier, B. Lee, N. Zelyas, and L. Chui. Shiga-toxigenic *Escherichia coli* detection in stool samples screened for viral gastroenteritis in Alberta, Canada. *J. Clin. Microbiol.*, **2011**, *49*, 574.
13. U. Käppeli, H. Hächler, N. Giezendanner, L. Beutin, and R. Stephan. Human infections with non-O157 Shiga toxin-producing *Escherichia coli*, Switzerland, 2000-2009. *Emerg. Infect. Dis.*, **2011**, *17*, 180.
14. C. R. Hermos, M. Janineh, L. L. Han, and A. J. McAdam. Shiga toxin-producing *Escherichia coli* in children: diagnosis and clinical manifestations of O157:H7 and non-O157:H7 infection. *J. Clin. Microbiol.*, **2011**, *49*, 955.
15. C. Ruan, L. Yang, and Y. Li. Immunobiosensor chips for detection of *Escherichia coli* O157:H7 using electrochemical impedance spectroscopy. *Anal. Chem.*, **2002**, *74*, 4814.
16. S. M. Radke, and E. C. Alocilja. A high density microelectrode array biosensor for detection of *E. coli* O157:H7. *Biosens. Bioelectron.*, **2005**, *15*, 1662.
17. Y. H. Lin, S. H. Chen, Y. C. Chuang, Y. C. Lu, T. Y. Shen, C.A. Chang, and C. S. Lin. Disposable amperometric immunosensing strips fabricated by Au nanoparticles-modified screen-printed carbon electrodes for the detection of foodborne pathogen *Escherichia coli* O157:H7. *Biosens. Bioelectron.*, **2008**, *23*, 1832.
18. Y. Li, P. Cheng, J. Gong, L. Fang, J. Deng, W. Liang, and J. Zheng. Amperometric

- immunosensor for the detection of *Escherichia coli* O157:H7 in food specimens. *Anal. Biochem.*, **2012**, *421*, 227.
19. X. L. Su, and Y. Li. A self-assembled monolayer-based piezoelectric immunosensor for rapid detection of *Escherichia coli* O157:H7. *Biosens. Bioelectron.*, **2004**, *19*, 563.
  20. J. Waswa, J. Irudayarajb, and C. DebRoy. Direct detection of *E. Coli* O157:H7 in selected food systems by a surface plasmon resonance biosensor. *LWT - Food Science and Technology*, **2007**, *40*, 187.
  21. Y. Wang, Z. Ye, and C. Si, Ying. Subtractive inhibition assay for the detection of *E. coli* O157:H7 using surface plasmon resonance. *Sensors*, **2011**, *11*, 2728.
  22. S. Bouguelia, Y. Roupioz, S. Slimani, L. Mondani, M. G. Casabona, C. Durmort, T. Vernet, R. Calemczuk, and T. Livache. On-chip microbial culture for the specific detection of very low levels of bacteria. *Lab. Chip.*, **2013**, *13*, 4024.
  23. A. D. Taylor, J. Ladd, Q. Yu, S. Chen, J. Homola, and S. Jiang. Quantitative and simultaneous detection of four foodborne bacterial pathogens with a multi-channel SPR sensor. *Biosens. Bioelectron.*, **2006**, *22*, 752.
  24. L. Mondani, S. Delannoy, R. Mathey, F. Piat, T. Mercey, S. Slimani, P. Fach, T. Livache, and Y. Roupioz. Fast detection of both O157 and non-O157 shiga-toxin producing *Escherichia coli* by real-time optical immunoassay. *Lett. Appl. Microbiol.*, **2015**, *62*, 39.
  25. S. K. Arya, A. Singh, R. Naidoo, P. Wu, M. T. McDermott, and S. Evoy. Chemically immobilized T4-bacteriophage for specific *Escherichia coli* detection using surface plasmon resonance. *Analyst.*, **2011**, *136*, 486.
  26. Y. Wang, Z. Ye, C. Si, and Y. Ying. Monitoring of *Escherichia coli* O157:H7 in food samples using lectin based surface plasmon resonance biosensor. *Food Chem.*, **2013**, *136*, 1303.
  27. E. Bulard, A. Bouchet-Spinelli, P. Chaud, A. Roget, R. Calemczuk, S. Fort, and T. Livache. Carbohydrates as new probes for the identification of closely related *Escherichia coli* strains

- using surface plasmon resonance imaging. *Anal. Chem.*, **2015**, 87, 1804.
28. Y. Morita, Denka Seiken Co., Ltd., Personal Communication, **2016**.
  29. Y. Iijima, N. T. Asako, M. Aihara, and K. Hayashi. Improvement in the detection rate of diarrhoeagenic bacteria in human stool specimens by a rapid real-time PCR assay. *J. Med. Microbiol.*, **2004**, 53, 617.
  30. M. L. Mangoni, R. F. Epand, Y. Rosenfeld, A. Peleg, D. Barra, R. M. Epand, and Y. Shai. Lipopolysaccharide, a key molecule involved in the synergism between temporins in inhibiting bacterial growth and in endotoxin neutralization. *J. Biol. Chem.*, **2008**, 283, 22907.
  31. Y. Nishiuchi, M. Doe, H. Hotta, and K. Kobayashi. Structure and serologic properties of O-specific polysaccharide from *Citrobacter freundii* possessing cross-reactivity with *Escherichia coli* O157:H7. *FEMS Immunol. Med. Microbiol.*, **2000**, 28, 163.
  32. Y. Hirakawa, T. Yamasaki, E. Watanabe, F. Okazaki, Y. Murakami-Yamaguchi, M. Oda, S. Iwasa, H. Narita, and S. Miyake. Development of an immunosensor for determination of the fungicide chlorothalonil in vegetables, using surface plasmon resonance. *J. Agric. Food Chem.*, **2015**, 63, 6325.
  33. Y. Hirakawa, T. Yamasaki, A. Harada, T. Ohtake, K. Adachi, S. Iwasa, H. Narita, and S. Miyake. Analysis of the fungicide boscalid in horticultural crops using an enzyme-linked immunosorbent assay and an immunosensor based on surface plasmon resonance. *J. Agric. Food Chem.*, **2015**, 63, 8075.
  34. G. C. Bokken, R. J. Corbee, F. van Knapen, and A. A. Bergwerff. Immunochemical detection of *Salmonella* group B, D and E using an optical surface plasmon resonance biosensor. *FEMS Microbiol. Lett.*, **2003**, 222, 75.
  35. S. Scarano, A. Vestri, M. L. Ermini, and M. Minunni. SPR detection of human hepcidin-25: a critical approach by immuno- and biomimetic-based biosensing. *Biosens. Bioelectron.*, **2013**, 40, 135.

36. L. Grosjean, B. Cherif, E. Mercey, A. Roget, Y. Levy, P. N. Marche, M. B. Villiers, and T. Livache. A polypyrrole protein microarray for antibody-antigen interaction studies using a label-free detection process. *Anal. Biochem.*, **2005**, *347*, 193.
37. S. Bellon, W. Buchmann, F. Gonnet, N. Jarroux, M. Anger-Leroy, F. Guillonneau, and, R. Daniel. Hyphenation of surface plasmon resonance imaging to matrix-assisted laser desorption ionization mass spectrometry by on-chip mass spectrometry and tandem mass spectrometry analysis. *Anal. Chem.*, **2009**, *81*, 7695.
38. M. B. Villiers, S. Cortès, C. Brakha, J. P. Lavergne, C. A. Marquette, P. Deny, T. Livache, and P. N. Marche. Peptide-protein microarrays and surface plasmon resonance detection: biosensors for versatile biomolecular interaction analysis. *Biosens. Bioelectron.*, **2010**, *26*, 1554.
39. I. Gutiérrez-Aguirre, V. Hodnik, L. Glais, M. Rugar, E. Jacquot, G. Anderluh, and M. Ravnikar. Surface plasmon resonance for monitoring the interaction of *Potato virus Y* with monoclonal antibodies. *Anal. Biochem.*, **2014**, *447*, 74.
40. R. Stenutz, A. Weintraub, and G. Widmalm. The structures of *Escherichia coli* O-polysaccharide antigens. *FEMS Microbiol. Rev.*, **2006**, *30*, 382.

**Chapter 3      Evaluation of a Surface Plasmon Resonance-Based Multiplex  
O-antigen Serogrouping for *Escherichia coli* using Eleven Major  
Serotypes of Shiga -Toxin-Producing *E. coli***

**Abstract**

The early detection of Shiga toxin-producing *Escherichia coli* (STEC) is important for early diagnosis and preventing the spread of STEC. Although the confirmatory test for STEC should be based on the detection of Shiga toxin using molecular analysis, isolation permits additional characterization of STEC using a variety of methods, including O:H serotyping. The conventional slide agglutination O-antigen serogrouping used in many clinical laboratories is laborious and time-consuming. Surface plasmon resonance (SPR)-based immunosensors are commonly used to investigate a large variety of bio-interactions such as antibody/antigen, peptide/antibody, DNA/DNA, and antibody/bacteria interactions. SPR imaging is characterized by multiplexing capabilities for rapidly screening (approximately 100 to several hundred sensorgrams in parallel) molecules. SPR-based O-antigen serogrouping method for STEC was recently developed by detecting the interactions between O-antigen-specific antibodies and bacterial cells themselves. The aim of this study was to evaluate its performance for *E. coli* serogrouping using clinical STEC isolates by comparing the results of slide agglutination tests. We tested a total of 188 isolates, including O26, O45, O91, O103, O111, O115, O121, O128, O145, O157, and O159. The overall sensitivity of SPR-based O-antigen serogrouping was 98.9%. Only two O157 isolates were misidentified as nontypeable and O121. The detection limits of all serotypes were distributed between  $1.1 \times 10^6$  and  $17.6 \times 10^6$  CFU/ml. Pulsed-field gel electrophoresis (PFGE) revealed the heterogeneity of the examined isolates. In conclusion, SPR is a useful method for the O-antigen serogrouping of STEC isolates, but the further evaluation of non-O157 minor serogroups is needed.

## Introduction

The O (somatic) polysaccharides and H (flagellar) surface antigens have been commonly used for *Escherichia coli* serotyping in epidemiological studies. Although more than 170 different O-antigen serogroups and 50 H-antigen types exist for *E. coli*, they are commonly used in surveillance and/or outbreak studies of *E. coli* associated infections including food born infections because the actual number of serotype combinations is limited.

Shiga toxin-producing *Escherichia coli* (STEC) is one of the most important pathogens in contaminated food<sup>1</sup>. Foodborne infections of STEC can cause large outbreaks with serious consequences, such as haemolytic uremic syndrome (HUS)<sup>1</sup>. In the United States, 465 STEC O157:H7 cases (0.95 per 100,000 population) with three deaths (0.6%) and 807 non-O157 STEC cases (1.65 per 100,000 population) with one death were reported by FoodNet in 2015 (<https://www.cdc.gov/foodnet/pdfs/FoodNet-Annual-Report-2015-508c.pdf>); thus, detecting both O157 and non-O157 STEC infections is necessary for management and control. Although the confirmatory test for STEC should be based on the detection of Shiga toxin using molecular analysis, isolation permits additional characterization of STEC using a variety of methods, including O:H serotyping.<sup>2</sup> The Centres for Disease Control and Prevention (CDC) recommend that all stools submitted for testing from patients with acute community-acquired diarrhoea should be cultured for O157 STEC on a selective and differential medium and that these stools should be simultaneously assayed for non-O157 STEC with a test that detects the Shiga toxins or the genes encoding these toxins.<sup>3,4</sup> However, these recommendations have not been adopted by all laboratories due to factors including the test quality, cost, clinical relevance for the patient population served, staffing, and technical expertise of the technologists.<sup>5</sup> Most O157 strains can be isolated using commercially available selective and differential agar media that take advantage of the fact that most of the strains do not utilize sorbitol or are 4-methylumbelliferly-

beta-D-glucuronidase (MUG)-negative after 24 h in culture.<sup>2</sup> However, no selective and differential media are available for the detection of non-O157 STEC strains. This lack is one reason why the CDC recommends that specimens or enrichment broths in which Shiga toxin or STEC is detected but from which O157 STEC is not recovered should be forwarded to a public health laboratory.<sup>4</sup> However, this protocol requires significant additional costs. Therefore, a system that can identify the representative serogroup producing Shiga toxin may support the sequential protocol for the identification of STEC.

Although various novel technologies based on PCR, ELISA, and whole-genome sequencing have been developed for the identification of *E. coli* O-antigen serotypes,<sup>6–11</sup> conventional slide agglutination O-antigen serogrouping is still used in many clinical laboratories. Agglutination typing is a simple method but is laborious and time consuming. In addition, the results could be ambiguous due to the variability in antisera production and a lack of standard methodology. Surface plasmon resonance (SPR)-based immunosensors are commonly used to investigate a large variety of bio-interactions such as antibody/antigen, peptide/antibody, DNA/DNA, and antibody/ bacteria interactions.<sup>12</sup> SPR imaging (SPRi) is characterized by its multiplexing capability to rapidly screen (approximately 100 to several hundred sensorgrams in parallel) molecules.<sup>13–15</sup> Despite their utility, the number of SPR and SPR studies of cells has been low compared to other biological systems because of the additional handling requirements and potential instrument contamination issues.<sup>12</sup>

Although more than 400 STEC serotypes have been identified, only a subset of O-antigen serogroups have been correlated with illness in humans.<sup>16</sup> The most common enterohemorrhagic *E. coli* (EHEC) strains identified as STEC belong to serogroups O157, O26, O45, O103, O111, O121 and O145 and cause haemorrhagic colitis and HUS.<sup>17–19</sup> Recently, a rapid and multiplex SPR-based O antigen serogrouping method for STEC was developed.<sup>20</sup> However, the clinical performance of this method for many clinical isolates has not yet been reported.

The aim of this study was to evaluate the performance of a SPR-based O-antigen serogrouping method for major STEC serotypes in Japan using clinical isolates.

## **Experimental**

### *Bacterial strains*

The STEC isolates that were investigated in this study were collected by two regional public health institutions, the Kobe Institute of Health (KIH) and Ehime Prefectural Institute of Public Health and Environmental Science (EPHES), from patients who were suspected of harbouring EHEC or from contaminated environments. The KIH and EPHES manage populations of 5.6 million and 1.4 million, respectively. The isolates were collected by the KIH between 1996 and 2015 and by EPHES between 1997 and 2015. Additionally, we purchased five standard strains (one O45 strain and four O103 strains) from the Research Institute for Microbial Diseases, Osaka University (RIMD). Conventional agglutination O antigen serogrouping for all isolates was performed using commercially available *E. coli* antisera (Denka Seiken Co. Ltd, Tokyo, Japan) as a reference for the O-antigen serotype.

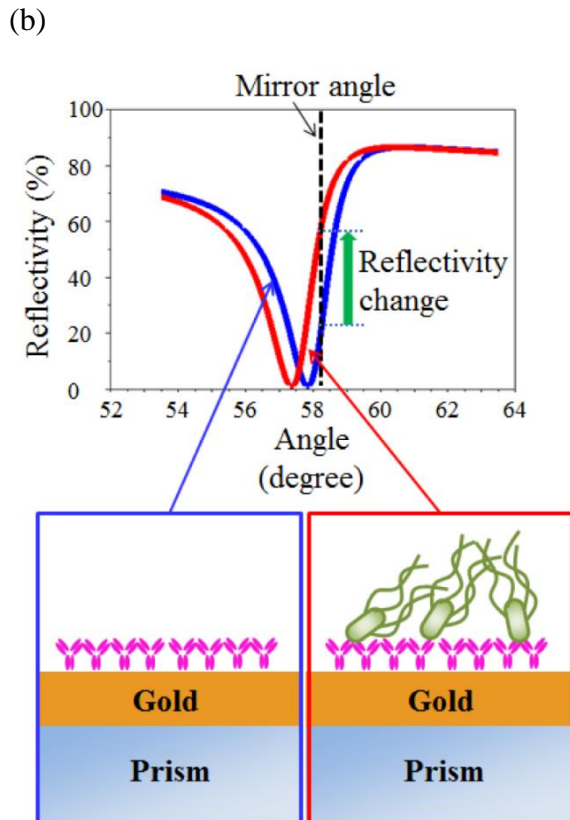
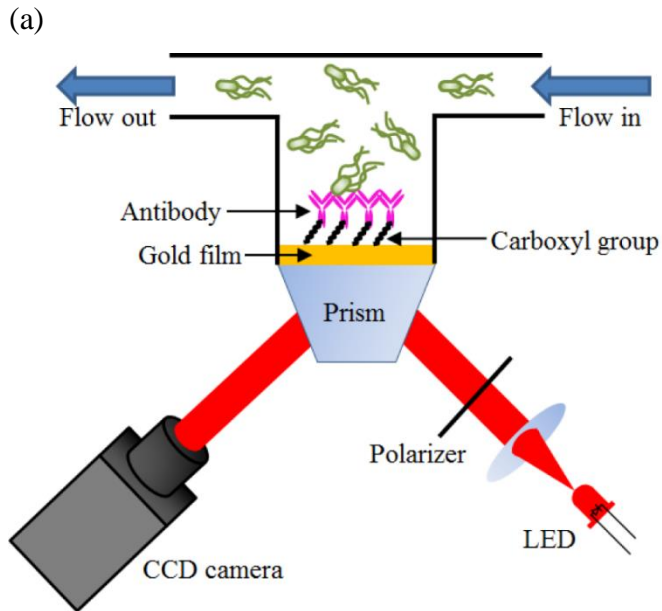
### *Identification of *stx1* and *stx2**

We confirmed the presence of the *stx1* and *stx2* genes by PCR as previously described.<sup>21</sup> The primers LP30 and LP31 were used to detect *stx1*, and the primers LP43 and LP44 were used to detect *stx2*.

### *SPR-based O-antigen serogrouping*

We performed O-antigen determination using an SPR instrument (OpenPlex [HORIBA Scientific, Ltd., Palaiseau, France]) as previously described.<sup>20</sup> The biochip consisted of a prism and a gold thin-layer, the surface of which was modified with molecules terminated in a

carboxyl group (CS-HD [HORIBA Scientific]) (Fig. 1).



(c)

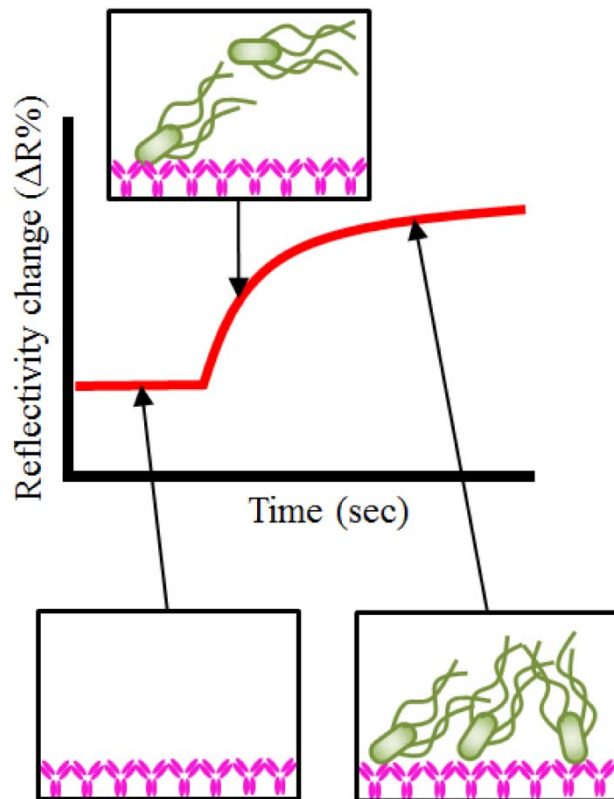


Fig. 1 Schematic of the SPR immunosensor used in this study. (a) The CCD camera monitored the refractive index changes that occurred when biomolecules (*Escherichia coli* O-antigen) were associated with O-antigen-specific antibodies immobilized on the surface of the gold film. The antibodies were immobilized on the gold surface using a carboxyl-terminated self-assembled monolayer. (b) When the bacterial cells attached to the antibodies, the refractive index at the surface changed, and the resonance angle shifted, causing an increase in reflectivity at a fixed incident light angle (mirror angle). (c) As more bacterial cells attached to the antibodies over time, the increase in the reflective change became larger.

### *SPR analysis preparation*

We purified the IgG antibody components of each of the *E. coli* O antigen serotypes (O26, O45, O91, O103, O111, O115, O121, O128, O145, O157 and O159) from commercially available *E. coli* O-antigen specific rabbit polyclonal antisera (Denka Seiken Co. Ltd, Tokyo, Japan) using protein G beads (GE Healthcare UK Ltd, Buckinghamshire, England) as previously described.<sup>20</sup> These 11 purified antisera and an anti-mouse immunoglobulin that was used as a negative control were individually spotted on the surface of a biochip. The details of spot condition were described previously.<sup>20</sup>

### *SPR analysis procedure*

Running buffer (PBS with 0.2% bovine serum albumin [BSA] and 0.02% Tween 20) continuously flowed through an SPR line at a rate of 50 ml/min. An examined isolate was suspended in PBS with 0.2% BSA and 0.02% Tween20 at 0.9–1.0 OD (530 nm). After injecting 200 ml of the bacterial cell suspension through the line, we measured the reactions between the bacterial cells and spotted antibodies for a maximum of 120 s. Gelatin gel (3%) was used to regenerate the sensor chip.

### *Identification of the O-antigen from the results of SPR analysis*

The bacterial samples were flowed in random order by an experimenter and an evaluator who did not know the sample information judged the real-time reaction curve and determined a serogroup of the tested isolates. The results of the tests were compared to the reference O-antigen serogroup determined by the conventional agglutination typing method to calculate the sensitivity and specificity of the novel methods.

### *Determination of the detection limits*

To identify the detection limits of the novel serogrouping methods, we created two-fold serial dilutions of the analyte suspension for each representative serotype starting from 0.97 to 1.03 OD (530 nm) to 0.5 to the ninth power. We prepared the same number of negative control samples, which contained only running buffer, as the number of serial dilutions; then, we measured the reactions of the dilutions and the negative control samples in a random order in a blinded manner. We repeated this sequence three times and determined the detection limit of the sample concentration at which the serogroup was identified correctly for all three sequences.

#### *Pulsed-field gel electrophoresis (PFGE)*

To confirm the heterogeneity of the examined isolates, we performed PFGE according to the CDC's PulseNet standard procedure using XbaI as the primary enzyme.<sup>22</sup> Half of the O26, O103, O121, O145, and O157 isolates were randomly selected for analysis. All the isolates of O91 and O111, which included two to nine isolates, were analysed.

## **Results**

#### *Isolate characteristics*

The isolate characteristics are summarized in Table 1. We examined a total of 188 isolates, which comprised 115, 68 and 5 isolates collected by the KIH, EPHEs and RIMD, respectively. The number of isolates of each O-antigen serotype was as follows: O157, 72; O26, 51; O121, 20; O103, 13; O145, 13; O111, 9; O91, 6; O45, 1; O115, 1; O128, 1; and O159, 1. Seventy-seven isolates contained both *stx1* and *stx2*, 74 isolates had only the *stx1* gene, and 37 isolates had only the *stx2* gene.

Table 1 Characteristics of the isolates examined in this study.

O-antigen type	Total No. of isolates	No. of <i>stx1</i> (+) and <i>stx2</i> (+)	No. of <i>stx1</i> (+) and <i>stx2</i> (-)	No. of <i>stx1</i> (-) and <i>stx2</i> (+)	No. of isolates collected by each institution (KIH:EPHES:RIMD)
26	51	17	34	0	11:40:0
45	1	0	1	0	0:0:1
91	6	4	2	0	2:4:0
103	13	13	0	0	3:6:4
111	9	4	5	0	4:5:0
115	1	0	1	0	1:0:0
121	20	1	0	19	19:1:0
128	1	1	0	0	1:0:0
145	13	3	6	4	11:2:0
157	72	46	12	14	62:10:0
159	1	1	0	0	1:0:0
Total	188	77	74	37	115:68:5

KIH: Kobe Institute of Health; EPHES: Ehime Prefectural Institute of Public Health and Environmental Science; RIMD: Research Institute for Microbial Diseases, Osaka University.

#### *SPR-based O-antigen serogrouping*

In total, 186 of 188 isolates (98.9%) were identified correctly (Table 2). The representative reaction curves are shown in Fig. 2. Except for O121 and O157, the sensitivity and specificity were 100% for all O-antigen serotypes. For the identification of O157 and O121, the sensitivity of O157 was 97.2% (70/72), and the specificity of O121 was 99.4% (167/168). One of the two misidentified O157 isolates did not react with any antibody spots. The other isolate reacted with both O157 and O121 spots. We prepared one biochip for this study, and the chip endured sequential analysis without a decrease in performance.

Table 2 Performance of STEC O-antigen typing with SPR for 11 major serotypes.

O-antigen type	No. of target isolates identified		No. of control isolates identified		Sensitivity (%)	Specificity (%)
	Total	Correctly identified	Total	Correctly identified		
26	51	51	137	137	100	100
45	1	1	187	187	100	100
91	6	6	182	182	100	100
103	13	13	175	175	100	100
111	9	9	179	179	100	100
115	1	1	187	187	100	100
121	20	20	168	167	100	99.4
128	1	1	187	187	100	100
145	13	13	175	175	100	100
157	72	70	116	116	97.2	100
159	1	1	187	187	100	100

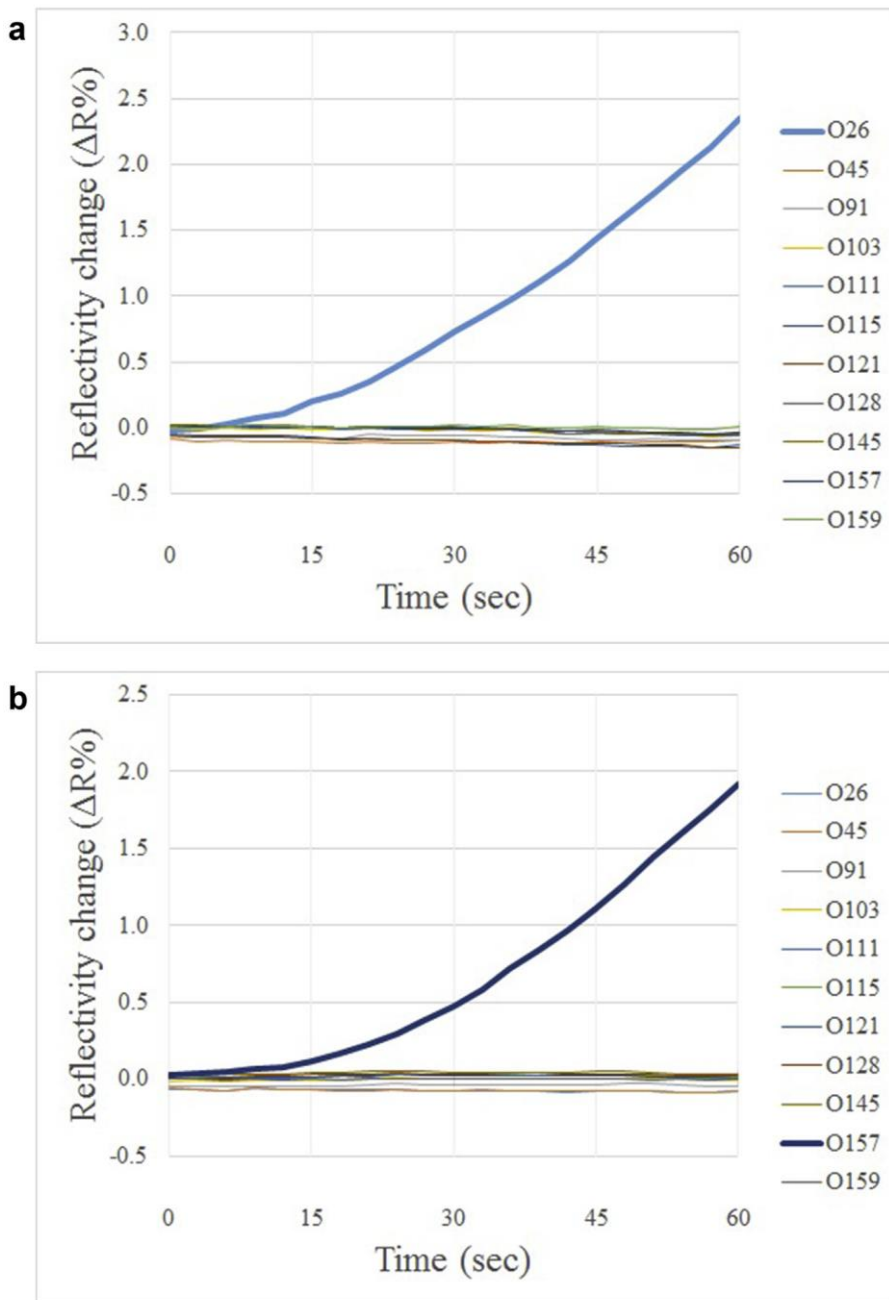


Fig. 2 Representative reaction curves for the examination of O26 (a) and O157 (b) isolates. In each analysis, only the corresponding antibody spot reacted with the O-antigen in of the flowing bacterial cells. The reaction increased the reflectivity by degrees starting from time 0, which corresponded to the time when the cells reached the sensor chip.

### Determination of the detection limits

All detection limits were distributed from  $1.1 \times 10^6$  to  $17.6 \times 10^6$  CFU/ml. The representative reaction curve is shown in Fig. 3. The detection limits of each serotype are as follows: O26,  $3.3 \times 10^6$ ; O45,  $1.1 \times 10^6$ ; O91,  $7.6 \times 10^6$ ; O103,  $11.0 \times 10^6$ ; O111,  $7.3 \times 10^6$ ; O115,  $5.7 \times 10^6$ ; O121,  $17.6 \times 10^6$ ; O128,  $13.4 \times 10^6$ ; O145,  $7.2 \times 10^6$ ; O157,  $7.6 \times 10^6$ ; and O159,  $10.1 \times 10^6$  CFU/ml.

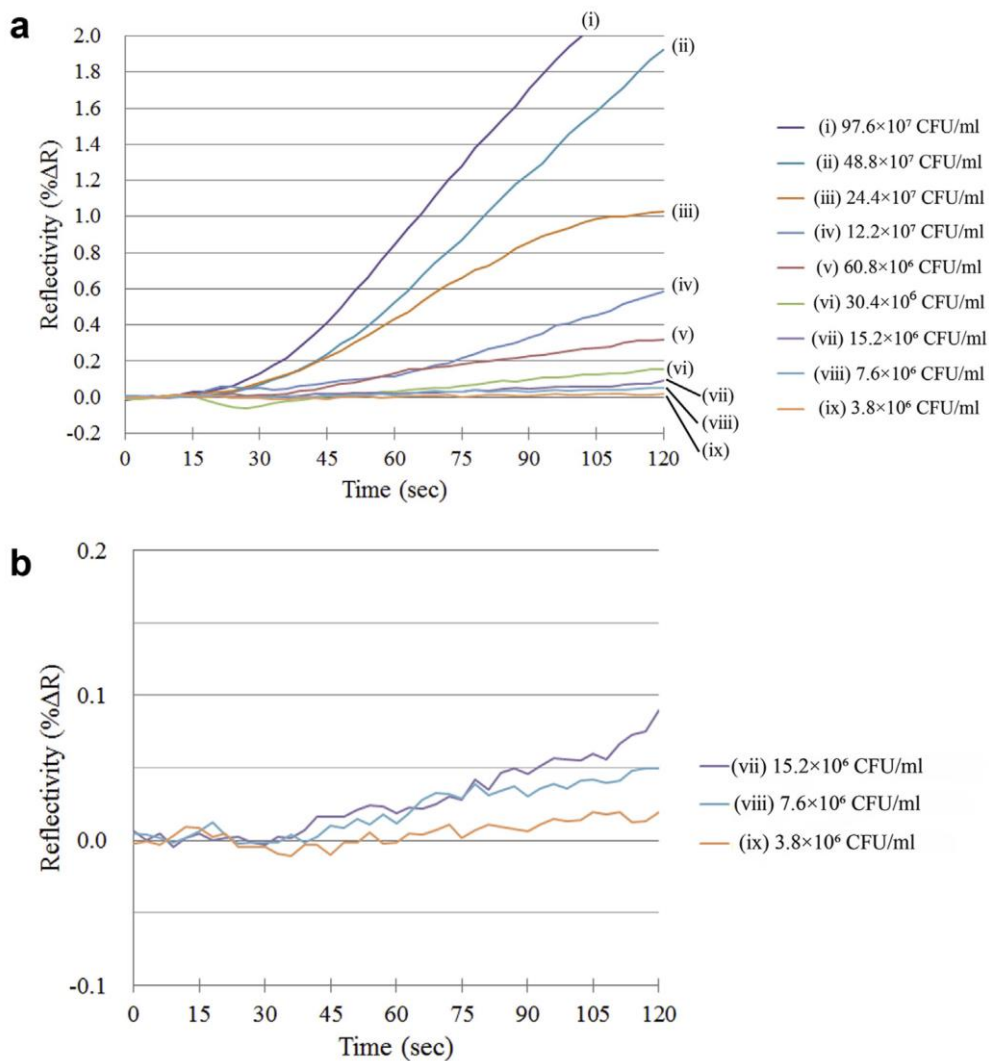


Fig. 3. The representative reaction curve used for the analysis of the detection limit of O157. (a) The reaction curve of each sample concentration. (b) The enlarged reaction curve of the samples with the three lowest concentrations.

*Molecular typing by PFGE*

All isolates, except the O157 and O26 isolates, exhibited different band patterns (Fig. 4). Based on an arbitrary similarity cut-off of 90%, this dendrogram classified a total of 101 tested isolates into 82 clusters, including 10 clusters with more than one isolate.

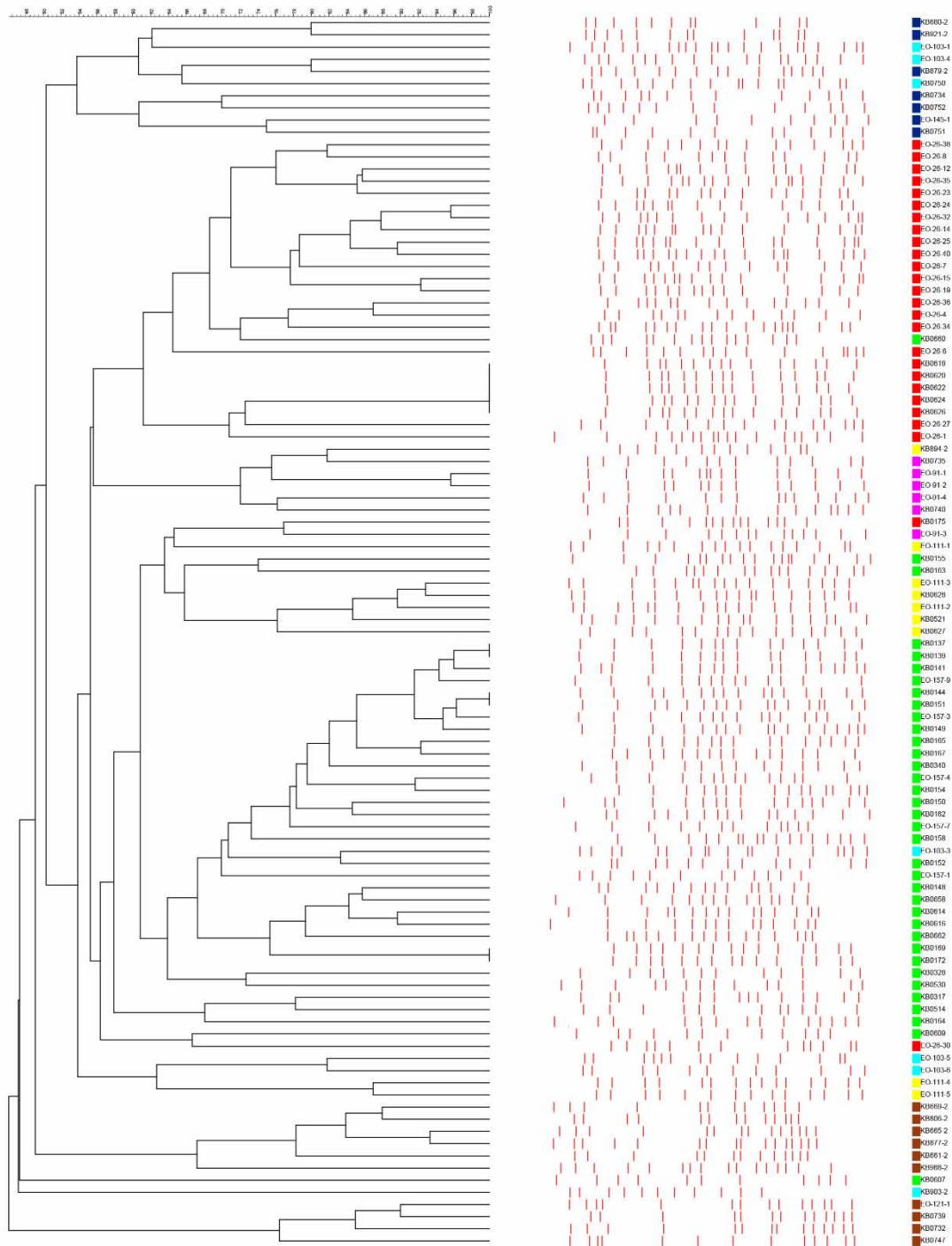


Fig. 4 Results of PFGE and similarity analysis of each O-antigen type with more than one isolate. The isolates with IDs that have the initials “KB” were collected by the Kobe Institute of Health, and the isolates with IDs that have the initials “EO” were collected by the Ehime Prefectural Institute of Public Health and Environmental Science. The initial colour of the square before each isolate name indicates the serotype of the isolate: red, O26; blue, O145; brown, O121; yellow, O111; pink, O91; light blue, O103; and green, O157.

## Discussion

In this study, we evaluated the performance of SPR-based *E. coli* O-antigen serogrouping using STEC isolates. For the 11 O-antigen serogroups of STEC that are prevalent in Japan, the identification rate, i.e., overall sensitivity, was 98.9%. In particular, for O157, which is the most prevalent EHEC globally, SPR had a high sensitivity of 97.2% and a specificity of 100%. Additionally, no cross-reactions were observed throughout the experiment, apart from one O157 isolate. Among the two isolates that were misidentified, one isolate did not react with any antibodies. The reaction of the O157-specific antisera for this isolate in the conventional agglutination assay was relatively weak, which might have led to the misidentification. Regarding the other misidentified isolate, a cross-reaction that was not identified in the conventional agglutination test but occurred in the SPR analysis might have caused the misidentification. The heterogeneity of the examined isolates indicated by the results of *stx* typing and PFGE analysis also support the utility of SPR-based *E. coli* O-antigen serogrouping. With regard to the detection limits, all O-antigen serotypes showed good detection limits between  $1.1 \times 10^6$  and  $17.6 \times 10^6$  CFU/ml. In general, the detection limit of SPR depends on the concentration of the analyte, the reaction period and the concentration of the material that is spotted on the chip. Therefore, the detection limits can be lowered by prolongation of the reaction period and increasing the concentration of the extracted IgG component.

SPR is a novel technology that can monitor a large variety of bio-interactions. SPR-based immunosensor applications for bacterial identification have been mainly based on monitoring DNA hybridization between bacterial DNAs and primers<sup>23-25</sup>, and applications using bacterial cells themselves have been limited. However, our study demonstrates that SPR-based immunosensors can be applied to bacterial identification based on monitoring the interaction between bacterial cells and antibodies. Although we assessed only 11 types of O-antigen serotypes in this study, this method can be applied to other serotypes of *E. coli*. In addition, because SPR applications can be flexibly modified from approximately 100-plex to several 100-plex, we can identify many more Oantigen serotypes in one test. This promising SPR performance would be helpful for the accurate diagnosis of STEC-related diarrhea resulting from isolates other than O157 and the ‘big six’ non-O-157 serotype isolates, which are not commonly tested in clinical laboratories. In addition, SPR may be used to identify *E. coli* O antigen serotypes in other situations, such as contaminated food surveillance and multi-drug-resistant *E. coli* surveillance.

Novel technologies for STEC O-antigen serogrouping, including PCR, real-time PCR, ELISA, and whole-genome sequencing, have recently been reported.<sup>6-11</sup> Compared to these technologies, SPR has several advantages. First, SPR-based analysis has great multiplicity. We can spot more than approximately 100 to several hundred materials on an SPR gold chip. Therefore, SPR can be used to identify large variety of factors at the same time. Although real-time-PCR based analysis and some types of immunoassays are compatible with multiplex analysis, SPR-based analysis has much greater multiplicity. Despite recent advances, whole-genome sequencing in microbiology remains expensive and requires specialized bioinformatics skills. In this aspect, SPR-based analysis is less expensive, simpler and easier to perform in clinical laboratories. In addition, SPR is more user-friendly than other molecular analysis-based methods because it does not require special skills, such as DNA extraction, which are

commonly needed for PCR and whole-genome sequencing. Second, SPR-based analysis can be applied to thickened samples such as liquid culture medium and gel.<sup>12,20</sup> This flexibility for samples allows the application to be flexible. For example, if observers use semisolid media or liquid media for the cultivation of the pathogen, the media could be directly injected into the instrument.

We should note a limitation in this study. Although we tested a total of 11 types of O-antigen serogroups, four O-antigen serogroups contained less than five isolates. In addition, many other *E. coli* serotypes can produce Shiga toxin. Therefore, to obtain more accurate sensitivity and specificity for all serogroups, further studies based on the collection of minor serogroup isolates are needed. However, we tested 72 O157 isolates and a total of 107 non-O157 “big six” serotype isolates, which are the prevalent serotypes throughout the world. According to the previous report from the CDC (<https://www.cdc.gov/foodnet/pdfs/FoodNet-Annual-Report-2015-508c.pdf>), the serotypes we tested covered more than 80% of the STEC infections in the USA in 2015. Therefore, the identification of these common O-antigen types of STEC would aid clinical practice. In addition, we believe that SPR is a promising method for the identification of other minor O-antigen serotypes of STEC because this application is based on the well-characterized interactions between *E. coli* cells and their specific antibodies.<sup>12</sup>

In conclusion, we evaluated the performance of SPR for the identification of the STEC O-antigen. We observed a 98.9% identification rate, which may be acceptable in a clinical laboratory. Further evaluation is needed to reveal the performance for minor O-antigen serotypes.

## References

1. M. A. Croxen, R. J. Law, R. Scholz, K. M. Keeney, M. Wlodarska, and B. B. Finlay. Recent advances in understanding enteric pathogenic *Escherichia coli*. *Clin Microbiol Rev*,

2013, 26, 822.

2. J. C. Paton, and A. W. Paton. Pathogenesis and diagnosis of Shiga toxin-producing *Escherichia coli* infections. *Clin Microbiol Rev*, **1998**, 11, 450.
3. L. H. Gould, C. Bopp, N. Strockbine, R. Atkinson, V. Baselski, B. Body, R. Carey, C. Crandall, S. Hurd, R. Kaplan, M. Neill, S. Shea, P. Somsel, M. Tobin-D'Angelo, P. M. Griffin, and P. Gerner-Smidt. Recommendations for diagnosis of shiga toxin-producing *Escherichia coli* infections by clinical laboratories. *MMWR Recommend Rep*, **2009**, 58, 1.
4. L. H. Gould. Update: recommendations for diagnosis of Shiga toxin-producing *Escherichia coli* infections by clinical laboratories. *Clin Microbiol Newsl*, **2012**, 34, 75.
5. M. J. Marcon. Point: should all stools be screened for Shiga toxin-producing *Escherichia coli*. *J Clin Microbiol*, **2011**, 49, 2390.
6. J. M. Carter, A. Lin, L. Clotilde, and M. Lesho. Rapid, multiplexed characterization of Shiga toxin-producing *Escherichia coli* (STEC) isolates using suspension array technology. *Front Microbiol*, **2016**, 7, 439.
7. A. Iguchi, S. Iyoda, K. Seto, T. Morita-Ishihara, F. Scheutz, and M. Ohnishi. *Escherichia coli* O-genotyping PCR: a comprehensive and practical platform for molecular O serogrouping. *J Clin Microbiol*, **2015**, 53, 2427.
8. Y. Hara-Kudo, N. Konishi, K. Ohtsuka, K. Iwabuchi, R. Kikuchi, J. Isobe, T. Yamazaki, F. Suzuki, Y. Nagai, H. Yamada, A. Tanouchi, T. Mori, H. Nakagawa, Y. Ueda, and J. Terajima. An interlaboratory study on efficient detection of Shiga toxin-producing *Escherichia coli* O26, O103, O111, O121, O145, and O157 in food using real-time PCR assay and chromogenic agar. *Int J Food Microbiol*, **2016**, 230, 81.
9. P. B. Shridhar, L. W. Noll, X. Shi, B. An, N. Cernicchiaro, D. G. Renter, T. G. Nagaraja, and J. Bai. Multiplex quantitative PCR assays for the detection and quantification of the six major non-O157 *Escherichia coli* serogroups in cattle feces. *J Food Prot*, **2016**, 79, 66.

10. K. G. Joensen, A. M. Tetzschner, A. Iguchi, F. M. Aarestrup, and F. Scheutz. Rapid and easy in silico serotyping of *Escherichia coli* isolates by use of whole-genome sequencing data. *J Clin Microbiol*, **2015**, *53*, 2410.
11. N. V. Hegde, R. Cote, B. M. Jayarao, M. Muldoon, K. Lindpaintner, V. Kapur, and C. Debroy. Detection of the top six non-O157 Shiga toxin-producing *Escherichia coli* O groups by ELISA. *Foodborne Pathog Dis*, **2012**, *9*, 1044.
12. P. N. Abadian, C. P. Kelley, and E. D. Goluch. Cellular analysis and detection using surface plasmon resonance techniques. *Anal Chem*, **2014**, *86*, 2799.
13. S. Cortes, C. L. Villiers, P. Colpo, R. Couderc, C. Brakha, F. Rossi, P. N. Marche, and M. B. Villiers. Biosensor for direct cell detection, quantification and analysis. *Biosens Bioelectron*, **2011**, *26*, 4162.
14. R. Bombera, L. Leroy, T. Livache, and Y. Roupioz. DNA-directed capture of primary cells from a complex mixture and controlled orthogonal release monitored by SPR imaging. *Biosens Bioelectron*, **2012**, *33*, 10.
15. M. B. Villiers, S. Cortès, C. Brakha, J. P. Lavergne, C. A. Marquette, P. Deny, T. Livache, and P. N. Marche. Peptide-protein microarrays and surface plasmon resonance detection: biosensors for versatile biomolecular interaction analysis. *Biosens Bioelectron*, **2010**, *26*, 1554.
16. M. Blanco, J. E. Blanco, A. Mora, G. Dahbi, M. P. Alonso, E. A. González, M. I. Bernárdez, and J. Blanco. Serotypes, virulence genes, and intimin types of Shiga toxin (verotoxin)-producing *Escherichia coli* isolates from cattle in Spain and identification of a new intimin variant gene (*eae-ξ*). *J Clin Microbiol*, **2004**, *42*, 645.
17. K. E. Johnson, C. M. Thorpe, and C. L. Sears. The emerging clinical importance of non-O157 Shiga toxin-producing *Escherichia coli*. *Clin Infect Dis*, **2006**, *43*, 1587.
18. J. T. Brooks, E. G. Sowers, J. G. Wells, K. D. Greene, P. M. Griffin, R. M. Hoekstra, and

- N. A. Strockbine. Non-O157 Shiga toxin-producing *Escherichia coli* infections in the United States, 1983-2002. *J Infect Dis*, **2005**, *192*, 1422.
19. Centers for Disease Control (CDC). Foodborne disease active surveillance network (FoodNet). *Atlanta: Centers for Disease Control*, **2016**.
  20. T. Yamasaki, S. Miyake, S. Nakano, H. Morimura, Y. Hirakawa, M. Nagao, Y. Iijima, H. Narita, and S. Ichiyama. Development of a surface plasmon resonance-based immunosensor for detection of 10 major O-antigens on Shiga toxin-producing *Escherichia coli*, with a gel displacement technique to remove bound bacteria. *Anal Chem*, **2016**, *88*, 6711.
  21. P. Feng, and S. R. Monday. Multiplex PCR for detection of trait and virulence factors in enterohemorrhagic *Escherichia coli* serotypes. *Mol Cell Probes*, **2000**, *14*, 333.
  22. S. B. Hunter, P. Vauterin, M. A. Lambert-Fair, M. S. Van Duyn, K. Kubota, L. Graves, D. Wrigley, T. Barrett, and E. Ribot. Establishment of a universal size standard strain for use with the PulseNet standardized pulsed-field gel electrophoresis protocols: converting the national databases to the new size standard. *J Clin Microbiol*, **2005**, *43*, 1045.
  23. B. P. Nelson, M. R. Liles, K. B. Frederick, R. M. Corn, R. M. Goodman. Label-free detection of 16S ribosomal RNA hybridization on reusable DNA arrays using surface plasmon resonance imaging. *Environ Microbiol*, **2002**, *4*, 735.
  24. J. Wang, Y. Luo, B. Zhang, M. Chen, J. Huang, K. Zhang, W. Gao, W. Fu, T. Jiang, and P. Liao. Rapid label-free identification of mixed bacterial infections by surface plasmon resonance. *J Transl Med*, **2011**, *9*, 85.
  25. Y. Xiang, X. Zhu, Q. Huang, J. Zheng, and W. Fu. Real-time monitoring of mycobacterium genomic DNA with target-primed rolling circle amplification by a Au nanoparticle-embedded SPR biosensor. *Biosens Bioelectron*, **2015**, *66*, 512.

## **Chapter 4      Specific Detection of c-Kit Expressed on Human Cell Surface by Immunosensor Based on Surface Plasmon Resonance**

### **Abstract**

Immunosensor based on surface plasmon resonance was developed for detection of c-Kit expressed on cell surface. The combination of the antibody solution modified with gelatin before immobilization to the sensor chip and its blocking with gelatin was drastically decreased the nonspecific reaction. The condition may be useful for the detection of various cells by using antibody against cell surface marker including the c-kit.

### **Introduction**

An immunosensor based on surface plasmon resonance (SPR) is direct detection method of antigen antibody interaction without any label of the antibody. The SPR immunosensor has been therefore applied to the detection of various mammalian cells, such as red blood cell,<sup>1,2</sup> lymphocyte,<sup>3,4</sup> corresponding cells of targeted therapy,<sup>5</sup> mesenchymal stem cells,<sup>6</sup> and virus-infected cells and tumor cells.<sup>7-9</sup>

The c-Kit is a receptor with tyrosine kinase that several types in the intracellular domain are known. It regulates proliferation, differentiation, and survival of cells through binding of the stem cell factor.<sup>10</sup> It is expressed on various kinds of cells including hematopoietic progenitor stem cells, mast cells, melanocytes, interstitial cells of Cajal, and germ cells.<sup>10-15</sup> Mutation of the genome proceeds to become to malignant tumor, such as gastrointestinal stromal tumors, testicular seminoma, melanoma, and acute myeloid leukemia.<sup>10,16-19</sup> Its inactivation proceeds to piebaldism.<sup>20</sup> They suggest that the c-Kit is important marker to monitor progress of their disease. The detection is generally carried out by a microscope observation or by a flow cytometer after reacted with fluorescence-labeled anti-c-Kit polyclonal antibody, while they are time-consuming

methods.

A microarray type immunosensor based on SPR has potential to detect simultaneously various cell surface markers. The purpose of this study is to examine the specific detection of c-Kit expressed on human cell surface by the immunosensor based on SPR with anti-c-Kit polyclonal antibody that reacts with outer cellular domain of all of the c-Kit type. This is a report of the result that the nonspecific reaction was drastically decreased by combination of the antibody solution modified with gelatin before immobilization to the sensor chip and its blocking with gelatin.

## **Experimental**

### *Materials*

Anti-c-Kit polyclonal antibody (goat IgG) crossly reacted with human and mouse c-Kit was purchased from R&D Systems, Inc. (Minnesota, USA). Nonspecific antibody (goat IgG) was purchased from Abcam plc (Cambridge, UK). RPMI-1640 medium, Dulbecco's modified Eagle's medium (DMEM), and bovine serum albumin (A7888; BSA) were purchased from Sigma-Aldrich Co. (St. Louis, MO, USA). Fetal bovine serum was purchased from Hyclone laboratories (South Logan, UT, USA). L-glutamine solution (200 mmol/L) was purchased from Fujifilm Wako Pure Chemical Corporation (Osaka, Japan). Penicillin and streptomycin sulfate were purchased from Life Technologies Corporation (Grand Island, NY, USA). Gelatin (fine powder), Dulbecco's phosphate-buffered saline without calcium and magnesium (PBS) and all other chemicals of analytical grade were purchased from Nacalai Tesque (Kyoto, Japan).

### *Cell culture*

Two kinds of the cell lines were provided from Horiba Ltd (Kyoto, Japan). Human megakaryoblastic leukemia cell line (MEG01s) and HEK293T cell line derived from kidney of human fetal was cultured in RPMI-1640 medium and DMEM, respectively, supplemented with

10% fetal bovine serum, L-glutamine (4 mmol/L), penicillin (100 units/mL), and streptomycin sulfate (100 µg/mL) under 5% CO<sub>2</sub> at 37 °C.

#### *Immunosensor construction*

The surface plasmon resonance imaging system (OpenPlex, Horiba Scientific, Palaiseau, France) and the sensor chip consisted on glass prism (CS-HD, Horiba Scientific), the carboxy group had been esterified with *N*-hydroxysuccinimide to bind antibodies, were used. The anti-c-Kit antibody and the nonspecific antibody were respectively diluted to 0.2 mg/mL with PBS. The antibody solutions were spotted onto the chip surface area (12 mm × 23 mm) at each 10 nL/spot using a spotter (Spot Master; Musashi Engineering, Tokyo, Japan) and was immediately stand at 4 °C for 16 h in 80% relative humidity. The chip surface was then washed 3 times with PBS. It was blocked with PBS containing BSA (10 mg/mL) at 25 °C for 1 h and was washed 3 times with PBS.

On the other hand, gelatin solutions (A: 1.0 mg/mL, B: 10 mg/mL) were dissolved at 80 °C in PBS and cooled down to 25 °C that they were not gelled. The anti-c-Kit antibody and the nonspecific antibody were respectively diluted to 0.2 mg/mL in PBS with the gelatin A. The antibody solutions were spotted and washed as well as the above. It was blocked with PBS containing BSA (10 mg/mL) or the gelatin B at 25 °C for 1 h and the excess proteins were removed by washing 3 times with PBS.

Unreacted carboxy groups were deactivated with ethanolamine solution (1 mol/L, adjusted to pH 8.5) for 30 min, and then washed 3 times with PBS. The antibody immobilized sensor chip was set into the instrument. The running buffer was prepared at the conditions: PBS containing BSA (2.0 mg/mL) and Tween20 (200 µg/mL) for the sensor chip blocked with BSA or PBS containing gelatin A and Tween20 (200 µg/mL) for the sensor chip blocked with gelatin B. The set sensor chip was rinsed with the running buffer at 25 µL/min until the SPR signal was stabilized.

#### *Detection of the c-Kit expressed on cell surface*

The cell suspensions were prepared at  $1 \times 10^7$  cells/mL with each of the running buffers. The cell suspension, each 200  $\mu$ L, was injected to the immunosensor, and flown at 25  $\mu$ L/min for 480 s. It was continuously changed to the running buffer, and was further flown at 25  $\mu$ L/min for 480 s. After detection of the signal from the bound cells, the sensor chip was regenerated with roughly crushed gelatin gel (30 mg/mL) at 25  $\mu$ L/min for 480 s, as described previously.<sup>21</sup> The sensor chip was reused for the next detection after the running buffer was flown.

#### **Results and Discussion**

Blocking of the sensor chip is an important step for specific detection by immunosensor. BSA was therefore used firstly as a blocking reagent in this study.<sup>5-9,21</sup> MEG01s, that c-Kit expression was well known, was injected to the immunosensor.<sup>22</sup> As shown in Fig. 1-A, the signal of anti-c-Kit antibody achieved to the highest intensity, 0.4%, at 480 s among the time course while the signal image of the spot was only emphasized a little compared to it with the nonspecific antibody, as shown in Fig. 1-C.

The nonspecific signal may be decreased by standing together in large number of much more hydrophilic protein among each of antibody molecule on the sensor chip as the working hypothesis. Gelatin that was chosen to the candidate was added to the antibody solution. The sensor chip after spotting the solution containing anti-c-Kit antibody and gelatin A was blocked with BSA or gelatin. The signal for MEG01s was not improved on the BSA blocking condition but drastically improved on the gelatin condition, as shown in Fig. 1-A. The signal was increased to 2.7% intensity at 480 s. The signal image of the anti-c-Kit antibody was also emphasized and it of the nonspecific antibody was not almost detected, as shown in Fig. 1-C.

The signal for HEK293T was not found on the sensor chip after spotting anti-c-Kit antibody

without addition of gelatin, as shown in Fig. 1-B. It was the reason that the cells bound on the anti-c-Kit antibody spot were almost the same number as them on the nonspecific antibody spot, as shown in Fig. 1-D. BSA would be easy to bind the major component of their cell surface commonly existing. It was reported that the c-Kit was slightly detected on HEK293T cell surface by flow cytometry analysis.<sup>23</sup> When the gelatin condition was applied to the HEK293T, the signal was found at 1.0% intensity, as shown in Fig. 1-B. The images of the anti-c-Kit antibody and the nonspecific antibody became clear as well as MEG01s, as shown in Fig. 1-D.

The cells, approximately more than 10  $\mu\text{m}$  diameter, show much larger size compared to the distance that the evanescent wave is reached. The detected signal must be mainly derived from the adhesive phase of the cell surface to the sensor chip.

The increased signal by the gelatin effect was rapidly decreased after switching the running buffer on 480 s and was converged to 2.3% - 2.4% intensity for MEG01s and 0.7% - 0.8% intensity for HEK293T. It was known that the c-Kit numbers by each cell was distributed among the range of 10 folds.<sup>23</sup> It was seemed that the minimum c-Kit expressed cells would be easily released from capture of the antibody to the liquid phase.

Gelatin effectively blocked nonspecific reaction of the cells and the c-Kit expressed cells could be specifically detected by the immunosensor based on SPR. It was considered that the gelatin contains large amount of associated water among each of its molecules, and the nonspecific reaction point of the cells surface may be minimized with the associated water. It was seemed that the gelatin is the suitable reagent for the cell detection. The condition found in this study may be useful for the detection of various cells by using antibody against cell surface markers.

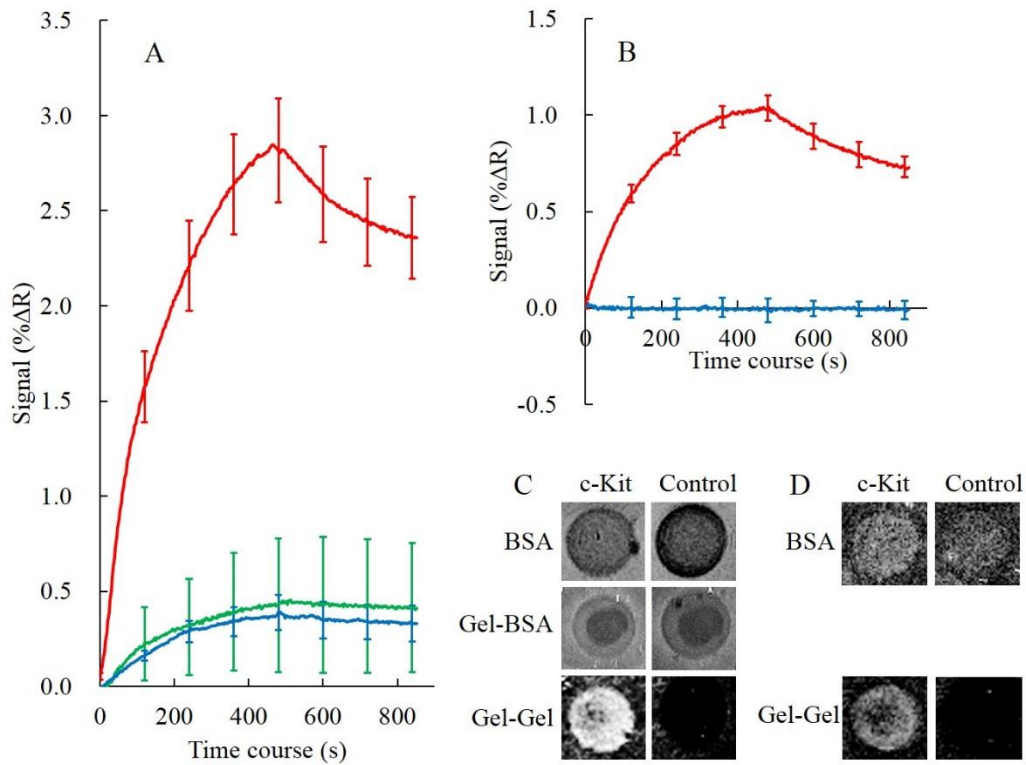


Fig. 1 Detection of c-Kit expressed on cell surface by immunosensor with BSA or gelatin. Time course of the reaction of immobilized anti-c-Kit antibody with MEG01s (A) and HEK293T (B). Blue line shows the results on the condition of immobilization of the antibody without gelatin and blocking of the sensor chip with BSA. Green line shows the result on the condition of antibody with gelatin and blocking with BSA. Red line shows the results on the condition of antibody with gelatin and blocking with gelatin. All lines are shown by the difference between signal intensity of anti-c-Kit antibody and it of nonspecific antibody. Each data point is the mean of 4 replicates in the same examination; error bars indicate  $\pm$  SD. SPR image of the reaction on 480 s from the MEG01s (C) and HEK293T (D). c-Kit shows the results with the anti-c-Kit antibody, and control shows the results with nonspecific antibody. BSA shows the results of the same condition as the above blue line. Gel-BSA shows the results of the same condition as the above green line. Gel-Gel shows the results of the same condition as the above red line.

## References

1. J. G. Quinn, R. O'Kennedy, M. Smyth, J. Moulds, and T. Frame. Detection of blood group antigens utilising immobilised antibodies and surface plasmon resonance. *J. Immunol. Methods*, **1997**, *206*, 87.
2. W. L. Then, M. I. Aguilar, and G. Garnier. Quantitative detection of weak D antigen variants in blood typing using SPR. *Sci. Rep.*, **2017**, *7*, 1616.
3. E. Suraniti, E. Sollier, R. Calemczuk, T. Livache, P. N. Marche, M. B. Villiers, and Y. Roupioz. Real-time detection of lymphocytes binding on an antibody chip using SPR imaging. *Lab Chip*, **2007**, *7*, 1206.
4. D. R. Baganizi, L. Leroy, L. Laplatine, S. J. Fairley, S. Heidmann, S. Menad, T. Livache, P. N. Marche, and Y. Roupioz. A simple microfluidic platform for long-term analysis and continuous dual-imaging detection of T-cell secreted IFN- $\gamma$  and IL-2 on antibody-based biochip. *Biosensors* [Basel], **2015**, *5*, 750.
5. D. Shanehbandi, J. Majidi, T. Kazemi, B. Baradaran, L. Aghebati-Maleki, F. Fathi, and J. E. N. Dolatabadi. Immuno-biosensor for detection of CD20-positive cells using surface plasmon resonance. *Adv Pharm Bull*, **2017**, *7*, 189.
6. Y. C. Kuo, J. H. Ho, T. J. Yen, H. F. Chen, and O. K. S. Lee. Development of a surface plasmon resonance biosensor for real-time detection of osteogenic differentiation in live mesenchymal stem cells. *PLoS One*, **2011**, *6*, e22382.
7. S. Cortès, C. L. Villiers, P. Colpo, R. Couderc, C. Brakha, F. Rossi, P. N. Marche, and M. B. Villiers. Biosensor for direct cell detection, quantification and analysis. *Biosens. Bioelectron.*, **2011**, *26*, 4162.
8. I. Janović, R. B. Schasfoort, and L. W. Mterstappen. Analysis of cell surface antigens by surface plasmon resonance imaging. *Biosens. Bioelectron.*, **2014**, *52*, 36.
9. A. Mendoza, D. M. Torrisi, S. Sell, N. C. Cady, and D. A. Lawrence. Grating coupled SPR

- microarray analysis of proteins and cells in blood from mice with breast cancer. *Analyst*, **2016**, *141*, 704.
10. J. Lennartsson, and L. Rönnstrand, Stem cell factor receptor/c-Kit: from basic science to clinical implications. *Physiol. Rev.*, **2012**, *92*, 1619.
  11. V. C. Broudy. Stem cell factor and hematopoiesis. *Blood*, **1997**, *90*, 1345.
  12. D. D. Metcalfe, D. Baram, and Y. A. Mekori. Mast cells. *Physiol. Rev.*, **1997**, *77*, 1033.
  13. M. A. Mackenzie, S. A. Jordan, P. S. Budd, and I. J. Jackson. Activation of the receptor tyrosine kinase Kit is required for the proliferation of melanoblasts in the mouse embryo. *Dev Biol*, **1997**, *192*, 99.
  14. J. D. Huizinga, L. Thuneberg, M. Klüppel, J. Malysz, H. B. Mikkelsen, and A. Bernstein, *Nature*, **1995**, *373*, 347.
  15. K. L. Loveland, and S. Schlatt. W/kit gene required for interstitial cells of Cajal and for intestinal pacemaker activity. *J. Endocrinol.*, **1997**, *153*, 337.
  16. JY. Blay. A decade of tyrosine kinase inhibitor therapy: Historical and current perspectives on targeted therapy for GIST. *Cancer Treat. Rev.*, **2011**, *37*, 373.
  17. J. W. Oosterhuis, and LH. Looijenga. Testicular germ-cell tumours in a broader perspective. *Nat. Rev. Cancer*, **2005**, *5*, 210.
  18. S. E. Woodman, and M. A. Davies. Targeting KIT in melanoma: a paradigm of molecular medicine and targeted therapeutics. *Biochem. Pharmacol.*, **2010**, *80*, 568.
  19. M. Malaise, D. Steinbach, and S. Corbacioglu. Clinical implications of *c-Kit* mutations in acute myelogenous leukemia. *Curr Hematol Malig Rep*, **2009**, *4*, 77.
  20. L. B. Giebel, and R. A. Spritz Proc. Mutation of the KIT (mast/stem cell growth factor receptor) protooncogene in human piebaldism. *Natl. Acad. Sci. U. S. A.*, **1991**, *88*, 8696.
  21. T. Yamasaki, S. Miyake, S. Nakano, H. Morimura, Y. Hirakawa, M. Nagao, Y. Iijima, H. Narita, and S. Ichiyama. Development of a surface plasmon resonance-based immunosensor

for detection of 10 major O-antigens on Shiga toxin-producing *Escherichia coli*, with a gel displacement technique to remove bound bacteria. *Anal. Chem.*, **2016**, 88, 6711.

22. Y. Sekido, T. Takahashi, R. Ueda, M. Takahashi, H. Suzuki, K. Nishida, T. Tsukamoto, T. Hida, K. Shimokata, K. M. Zsebo, and T. Takahashi. Recombinant human stem cell factor mediates chemotaxis of small-cell lung cancer cell lines aberrantly expressing the c-kit protooncogene. *Cancer Res.*, **1993**, 53, 1709.
23. C. Bahlawane, M. Schmitz, E. Letellier, K. Arumugam, N. Nicot, P. V. Nazarov, and S. Haan. Insights into ligand stimulation effects on gastro-intestinal stromal tumors signalling. *Cellular Signalling*, **2017**, 29, 138.

## List of publications

### Chapter 1

- Development of an Immunosensor Based on Surface Plasmon Resonance for Simultaneous Residue Analysis of Three Pesticides -Boscalid, Clothianidin, and Nitenpyram- in Vegetables.  
Hirakawa Y, Yamasaki T, Harada A, Iwasa S, Narita H, Miyake S  
Analytical sciences: the international journal of the Japan Society for Analytical Chemistry  
34(5) 533-539 (2018)

### Chapter 2

- マイクロアレイ型表面プラズモン共鳴センサーによる大腸菌 O 抗原の免疫測定方法の開発  
山崎 朋美, 森村 皓之, 中野 哲志, 三宅 司郎, 飯島 義雄, 長尾 美紀, 一山 智  
日本分析化学会年会講演要旨集 2015 年 8 月 26 日
- Development of a Surface Plasmon Resonance-Based Immunosensor for Detection of 10 Major O-Antigens on Shiga Toxin-Producing *Escherichia coli*, with a Gel Displacement Technique to Remove Bound Bacteria.  
Yamasaki T, Miyake S, Nakano S, Morimura H, Hirakawa Y, Nagao M, Iijima Y, Narita H, Ichiyama S  
Analytical chemistry 88(13) 6711-6717 (2016)

### Chapter 3

- SPRi(Surface Plasmon Resonance imaging)を用いた志賀毒素産生大腸菌のO抗原型決定

中野 哲志, 山崎 朋美, 山本 正樹, 松村 康史, 長尾 美紀, 高倉 俊二, 三宅 司郎, 一山 智

臨床病理 64(suppl): 240 -240 (2016)
- Evaluation of a Surface Plasmon Resonance Imaging-Based Multiplex O-Antigen Serogrouping for *Escherichia coli* using Eleven Major Serotypes of Shiga -Toxin-Producing *E. coli*.

Nakano S, Nagao M, Yamasaki T, Morimura H, Hama N, Iijima Y, Shinomiya H, Tanaka M, Yamamoto M, Matsumura Y, Miyake S, Ichiyama S

Journal of infection and chemotherapy: official journal of the Japan Society of Chemotherapy 24, 443-448 (2018)

#### Chapter 4

- Specific Detection of c-Kit Expressed on Human Cell Surface by Immunosensor Based on Surface Plasmon Resonance

Miyake S, Irikura D, Yamasaki T

Analytical sciences: the international journal of the Japan Society for Analytical Chemistry (2018) in press

## Acknowledgement

I am deeply grateful to Dr. Hajime Hatta, Professor of Kyoto Women's University, for giving me the opportunity for taking a doctoral degree.

I am deeply grateful to Dr. Hiroshi Narita, Professor Emeritus of Kyoto Women's University, for giving me the opportunity for taking a doctoral degree and his eager guidance, valuable discussions and helpful suggestions. He led me to a researcher.

I would also like to express my gratitude to Dr. Shiro Miyake, Professor of Azabu University, for his guidance in all this study and his persistent help. He also led me to a researcher.

I received generous support and technical guidance from Dr. Yuki Hirakawa, Researcher of Kyoto Women's University. I would like to express my gratitude to her.

I am grateful to Dr. Satoshi Ichiyama, Dr. Miki Nagao, and Dr. Satoshi Nakano, Kyoto University Hospital, for their professional support in the clinical field in Chapter 2 of this study. Without their research and publication, Chapter 3 of this study would not have been possible.

I would like to express the deepest appreciation to Dr. Yoshio Iijima, Kobe Institute of Health, for offering the strain of STEC and professional advice.

I am grateful to Dr. Hiroyuki Morimura and Dr. Daisuke Irikura, Horiba Ltd., for their technical support about SPR instrument.

I would like to offer my special thanks to Ms. Fumi Hirai, Ms. Asako Yamaguchi, Ms. Kaede Hirano, Ms. Natsuki Kawai, and members of Laboratory Foods, Kyoto Women's University, for their assistance.

I would like to thank to members of Kyoto Integrated Science & Technology Bio-Analysis Center for helpful suggestions and warm encouragement. Chapter 1 and Chapter 2 of this study were partially funded by the Aichi Science and Technology Foundation and by the Kyoto Integrated Science & Technology Bio-Analysis Center.

Finally, I am deeply grateful to professors of Department of Food and Nutrition of Kyoto Women's University.